Charles University in Prague

Faculty of Pharmacy in Hradec Králové

Department of Pharmacology and Toxicology

&

University of Porto

Faculty of Pharmacy

Department of Pharmacology

HISTONE DEACETYLASE INHIBITION AND MITOCHONDRIAL TRAFFICKING IN LIVING NEURONS

diploma thesis

Supervisors: Prof. Doutor Jorge Miguel de Ascenção Oliveira

Doc. PharmDr. Petr Pávek, Ph.D.

Porto, 2009   Iva Prokopová

Acknowledgements

I gratefully thanks to Prof. Jorge Oliveira for the possibility to work with him on this project, for his valuable pieces of advice, professional and kind supervising and reviewing of the manuscript. I thank to University of Porto for all the care and support for Erasmus students, my co-workers and all the laboratory team for everyday help and pleasant atmosphere during my stay at the university.

My sincere thanks go also to Doc. Petr Pávek and all PhD students in the Department of Pharmacology UK for accepting me in the working group, kindly helping me with the procedures before this project and teaching me the experimental work.

Declaration

I declare that this thesis is my original work, which I developed independently. All literature and other resources from which I drew in the processing, are listed in the references and were properly cited.

1 Abstract

Histone Deacetylase Inhibition and Mitochondrial Trafficking in Living Neurons

Mitochondrial trafficking is necessary for proper neuronal function and its impairment leads to neurodegeneration. We have found significant differences in mitochondrial movement between cortical and striatal neurons derived from rat brain. In striatum, mitochondria move with lower average speeds and decreased overal mitochondrial dynamics than those in cortex, exhibiting the same mitochondrial fractional occupancy in neuronal processes. How this could contribute to high striatal vulnerability in neurodegeneration is discussed. We used two different methods of trafficking analysis: manual and semi-automatic. These analyses determine average movement speeds of single mitochondria, as well as overal mitochondrial dynamics in particular field. Only neurons with established synaptic connections were analyzed, mitochondria travelling in both directions were found to move with equivalent average speeds, thus not further distinguished. Our preliminary results also reveal that histone deacetylase inhibition with trichostatin A increases mitochondrial trafficking in striatal neurons, independently of mitochondrial fractional occupancy and Ca^{2+} levels in neuronal processes. We suggest that possible mechanism of this effect is the selective inhibition of α-tubulin deacetylation.

Inhibice histon deacetyláz a mitochondriální pohyb v neuronech

Mitochondriální pohyb je nezbytný pro správnou funkci neuronů a jeho narušení vede k neurodegeneraci. Podařilo se nám nalézt signifikantní rozdíly v pohybu mitochondrií mezi neurony striata a cortexu, získanými z mozku potkanů. Ve striatu se mitochondrie pohybují nižšími průměrnými rychlostmi a se sníženou celkovou dynamikou v porovnání s cortexem, přičemž zaujímají stejnou frakční okupaci nervových výběžků. V diplomové práci je diskutováno, jak tento fakt může přispět ke zvýšené náchylnosti k neurodegeneraci buněk striata. Použili jsme dvě různé metody analýzy mitochondriálního pohybu: manuální a polo-automatickou. Tyto metody dokáží určit průměrné rychlosti jednotlivých mitochondrií stejně jako celkovou dynamiku mitochondrií v určité sledované oblasti. Analyzovali jsme pouze neurony s vytvořenými synaptickými propojeními, mitochondrie se pohybovaly v obou směrech stejnými průměrnými rychlostmi, proto nebyly dále rozlišovány dle směru pohybu. Naše předběžné výsledky také odhalily, že inhibice histon deacetyláz pomocí trichostatinu A zvyšuje pohyb mitochondrií v neuronech striata, nezávisle na mitochondriální frakční okupaci a hladině Ca^{2+} ve výběžcích neuronů. Předpokládáme, že pravděpodobným mechanismem vzrůstu dynamiky mitochondrií je selektivní inhibice deacetylace α-tubulinu.

2 Table of contents

3 Abbreviations list

ALS   Amyotrophic lateral sclerosis

AD   Alzheimer's disease

BDNF   Brain-derived neurothrophic factor

CNS   Central nervous system

ER   Endoplasmatic reticulum

FXS   Fragile X syndrom

HDAC   Histone deacetylase

HDACi   Histone deacetylase inhibitor(s)

HAT   Histone acetylase

HD   Huntington's disease

HDACi   Histone deacetylase inhibitor(s)

IC   Inhibition concentration

NGF   Neuronal growth factor

NMDA   N-methyl-D-aspartate

NPC   Niemann-Pick type C disease

PB   Phenyl butyrate

PD   Parkinson's disease

polyQ   Polyglutamine

ROI   Regions of interest

ROS   Reactive oxygen species

RSTS   Rubinstein-Taybi syndrome

SAHA   Suberoylanilide hydroxamic acid, also known as vorinostat

SB   Sodium butyrate

SBMA   Spinal and bulbar muscular atrophy

SIRT   Sirtuin

SMA   Spinal muscular atrophy

SMN   Survival motor neuron

TSA   Trichostatin A

VPA   Valproic acid

X-ALD   X-linked adrenoleukodystrophy

4 Introduction

Histone deacetylase inhibitors (HDACi) are a novel group of compounds presently undergoing clinical trials for its therapeutic application in a broad range of human disorders. They are mostly applied in cancer treatment for its ability to retain acetylation of histones, a mechanism frequently involved in the genesis of cancer. Nevertheless, recent studies have revealed potential therapeutic effects of HDACi on central nervous system disorders as well. These findings suggest that not only histone acetylation, but also non-histone substrate acetylation (for example α-tubulin) could be one of the targets modulating neurodegeneration in humans (Zhang et al., 2003).

Brain mitochondrial dysfunction is a major contributor to aging and neurodegenerative diseases. The effective maintenance of energy generation, regulation of apoptosis, and handling of toxic stimuli (e.g. increased calcium levels or reactive oxygen species), all these functions are influenced by mitochondrial biogenesis, trafficking and degradation. Recent studies evidence that neurodegenerative changes in particular areas of the brain are associated with mitochondrial trafficking and transportation defects (Dompierre et al., 2007; Trushina et al., 2004).

Our aim was to explore mitochondrial trafficking under physiological conditions trying to understand why striatal neurons are more vulnerable to Huntington's disease and other injuries than cortical neurons (Calabresi et al., 2000). More specifically, we assessed whether these neurons differ in mitochondrial fractional occupancy, trafficking speed, and Ca^{2+} levels in neuronal processes. Moreover, we tested whether a representative HDAC inhibitor (trichostatin A; TSA) modifies trafficking in cortical or striatal neurons. We hypothesized that by improving mitochondrial trafficking, HDAC inhibitors could influence the ability of neurons to cope with toxic stimuli and contribute to neuroprotection.

In our experiments, we treated cells with TSA which represents the HDAC inhibitors with hydroxamic acid structure. TSA acts as non-selective HDAC inhibitor and increases histone acetylation as well as acetylation of α-tubulin, essential protein involved in mitochondrial movement apparatus. This well-established experimental drug is very potent already at low nanomolar doses, moreover our laboratory has

previous experience with adequate acetylation ability and activity of TSA on striatal cells in Huntington's disease models (Oliveira et al., 2006).

Experiments were preformed with primary neuronal cultures using rat embryonic brains and the particular regions (cortex or striatum) were tested within physiological conditions or with addition of HDACi. Real time fluorescence videomicroscopy was used to record living neurons at the resolution of single mitochondrion.

To measure mitochondrial trafficking, we used two different strategies: manual tracking and semi-automatic analysis of the projections. These two strategies allow us to determine and calculate average mitochondrial speeds, as well as general dynamic of all mitochondria in the field.

5 Theoretical part

5.1 Mitochondria

5.1.1 Significance of mitochondria for neurons

Neurons

Neurons are highly specialized cells with richly branched and extensive processes, which can be as long as one meter in humans. Neurons possess sites with large demands for ATP and local $[Ca^{2+}]_i$ regulation, such as synapses, which are distributed throughout the length of axons and dendrites. This, along with constant remodeling of synaptic connections and related recruitment of vesicles and receptors, as well as the removal and degradation of synaptic proteins, present a dynamically changing demand for mitochondria (Chang and Reynolds, 2006b), (Fig.1.)

Corticostriatal projecting neurons have an essential role in transport of brain-derived neurotrophic factor (BDNF), a nerve gowth factor that support the survival of existing neurons and encourage the growth and differentiation of new neurons and synapses (Acheson et al., 1995; Dompierre et al., 2007).

The selective death of medium spiny neurons in the neostriatum in dependence to Huntington´s disease (HD), a devastating neurodegenerative disorder, proves their particular vulnerability to neurodegeneration (Rosas et al., 2008). On the other hand, cortical neurons in our experiments represent the more resistant region in the matter of neurodegeneration but since topologically selective, early, and progressive changes in the cortex has been described as well (Rosas et al., 2008), the characterization of mitochondrial dynamics is also adressed there.
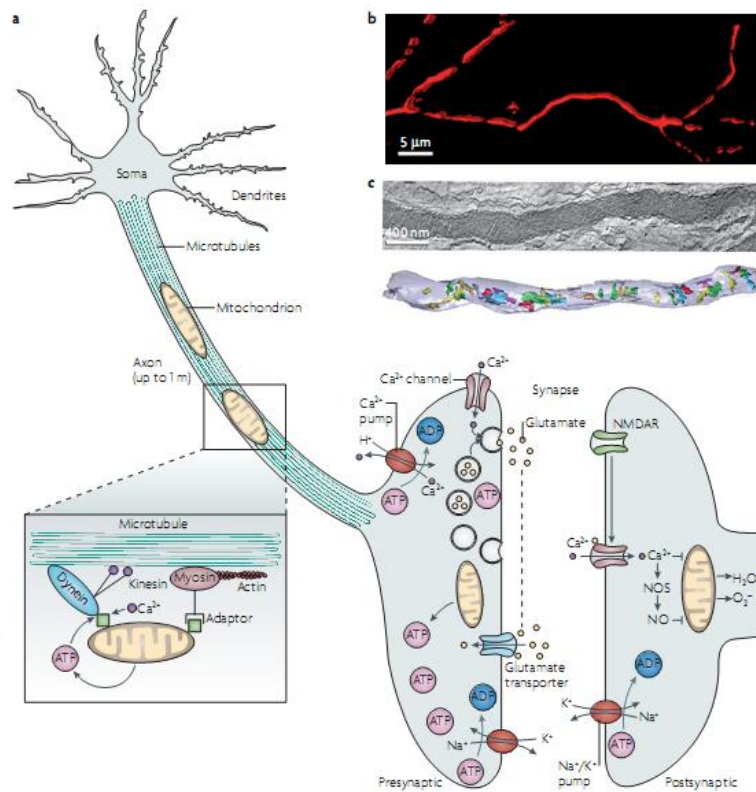
Figure 1. Neuronal mitochondria. a) Neurons require energy to transport organelles and cargo along microtubules or actin fibres (this process is mediated by motor molecules, such as dyneins, kinesins and myosin) and to maintain ion gradients and the membrane potential with ATP-dependent Ca^{2+} and Na^+/K^+ pumps and ion channels. At presynaptic terminals, neurotransmitter-vesicle is loading and Ca^{2+} -mediated neurotransmitter releases into the synaptic cleft. These events are also ATP-dependent. Glutamate re-uptake from the synaptic cleft is mediated by glutamate transporters and its post-synaptic binding to N-methyl-D-aspartate (NMDA) receptors evokes Ca^{2+} influx, which in turn can activate nitric oxide synthase (NOS) and stimulate the generation of nitric oxide (NO). Both NO and Ca^{2+} can directly modulate mitochondrial function by altering the levels of reactive oxygen species (H_2O_2 and O_2^-) and ATP production.

b) A fluorescence three-dimensional microscope image of mitochondria in a dendritic arbor of a neuron expressing a red fluorescent fusion protein that is targeted selectively to the mitochondrial matrix.

c) The top panel shows a slice through a mitochondrion in a neuronal process, as seen using electron tomography. The bottom panel shows a view of the surface-rendered volume after segmentation of the same mitochondrion. The outer membrane is a translucent pale blue and individual cristae are shown in different colours (Adapted from Knott et al., 2008).

Origin of mitochondria

Mitochondria (Fig.2) in present eukaryotic organisms developed from its descendants - mitochondrion and the plastid, two organelles creating endosymbiotic

(eu)bacteria, approximately 1.5×10^9 years ago. Mitochondria provided energy production whereas host cell synthesized proteins and ensured transcription (Gray, 1993). With its 37 genes, mammalian mitochondrial genome encodes only 13 proteins - for electron transport chain and oxidative phosphorylation (Garesse and Vallejo, 2001). Over 1000 additional proteins are encoded by the genes in the cell nucleus and mediate processes such as the regulation of ion homeostasis, stress responses, cell survival, and signal transduction (Mattson, 2008).
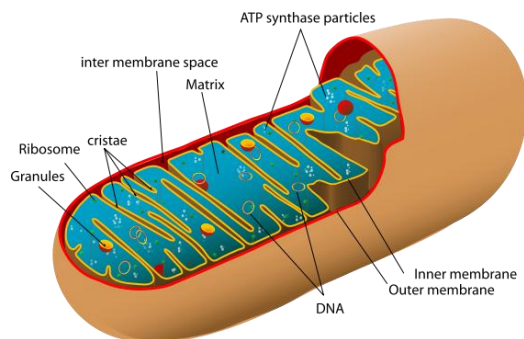
Figure 2 Structure of mitochondrion
(available at <http://commons.wikimedia.org/wiki/Mitochondrion>)

Energy generation

Mitochondria play an essential role in generating cellular energy, therefore being described as the "energy powerhouse of the cell". Proteins in the inner mitochondrial membrane – the electron transport chain - utilize O_2 and substrates such as glucose and pyruvate to produce cellular energy in the form of ATP. By coupling electron transport to the generation of proton gradients for oxidative phosphorylation, mitochondria produce approximately 15 times more ATP from glucose than the glycolytic pathway in eukaryotic cells (Chang and Reynolds, 2006b).

Cells of highly metabolic tissues such as muscle, liver and brain, are particularly dependent on mitochondria. Mitochondria can be found in huge density around the base of sperm flagella to power motility (Cardullo and Baltz, 1991), nested in the myofibrils of cardiac muscle facilitating contraction (Segretain et al., 1981), or rightly in brain which consumes 20% of resting metabolic energy while only comprising 2% of total body mass (Silver and Erecinska, 1998). Mitochondria supply over 95% of brain ATP

demand, mainly used to maintain Na^+, K^+ and Ca^{2+} ionic gradients (Silver and Erecinska, 1994), being most prevalent in regions of high metabolic demand, including synapses, nodes of Ranvier and myelination/demyelination interfaces (Chang and Reynolds, 2006b).

Loss of oxidative ATP production can be compensated independently of the mitochondria by glycolytic ATP synthesis. However, during severe anoxia and ischemia glycolytic ATP synthesis is insufficient to supply energetic needs, and disruption of mitochondrial function leads to consequential bioenergetic failure and necrotic cell death (Ankarcrona et al., 1995).

Many neurodegenerative diseases are associated with mitochondrial bioenergetic defects. In Alzheimer disease (AD), accumulation of full length amyloid precursor protein known to be the source of the toxic amyloid beta peptide, causes mitochondrial dysfunction and impaired energy metabolism, depolarizes mitochondria and promotes cytochrome c release and apoptosis (Anandatheerthavarada et al., 2003; Chang and Reynolds, 2006b). Parkinson's disease (PD) is associated with complex I deficiency (Schapira et al., 1989; Testa et al., 2005), mitochondrial respiration and ATP production are significantly reduced in Huntigton's disease (HD) cells (Milakovic and Johnson, 2005), and studies in amyotrophic lateral sclerosis (ALS) tissues and mutant models of ALS reveal loss of mitochondrial membrane potential ($\Delta\psi_m$), reduced mitochondrial mass, decreased activity of the mitochondrial DNA (mtDNA)-encoded cytochrome c oxidase enzyme and increased susceptibility to mitochondrial toxins (Chang and Reynolds, 2006b).

Ca^{2+} handling

Ca^{2+} is perhaps the most versatile intracellular messenger for all processes important to cellular function. It couples excitation to contraction, secretion, vesicle trafficking, cell proliferation, fertlization, metabolism, gene transcription, controls enzyme activity through protein phosphorylation-dephosphorylation, regulates ion channels, but also transmits signals that promote apoptosis and when escaping control, Ca^{2+} precipitates toxic cell death (Carafoli et al., 2001). Recent evidence also reveals that Ca^{2+} regulate mitochondrial motility through kinesin motor domain. Additionally, oxidative phosphorylation and ATP synthesis during times of high cellular demand can

be regulated by Ca^{2+}-sensitive dehydrogenase (McCormack and Denton, 1980). Thus disruption of calcium homeostasis diminishes neuronal resistance to excitotoxicity (Wang and Schwarz, 2009).

Regulating calcium homeostasis is a fundamental property of mitochondria, serving as "cytosolic buffers" for calcium. Mitochondria are able to buffer $[Ca^{2+}]_i$ by virtue of their negatively charged mitochondrial membrane potential (ψ_m) and low $[Ca^{2+}]_{mito}$ relative to the $[Ca^{2+}]_i$. Uptake of Ca^{2+} into the mitochondrial matrix is electrochemically favored, and is largely accomplished through the Ca^{2+}-uniporter. Mitochondrial Ca^{2+} sequestration is reversible, with Ca^{2+} efflux back into the cytosol occurring through the mitochondrial Na^+/ Ca^{2+} exchanger. Ca^{2+} release from mitochondria can prolong elevated $[Ca^{2+}]_i$, mediating important physiological functions such as excytosis and post-tetanic potentiation at presynaptic terminals (Chang and Reynolds, 2006b; Crompton et al., 1978). In addition, mitochondria interact with the endoplasmic reticulum (ER), both physically and functionally. ER and mitochondria bidirectionally exchange Ca^{2+}, supporting cell metabolism, signaling, and even cell death (Mironov and Symonchuk, 2006; Pizzo and Pozzan, 2007).

There are many harmful consequences connected with insufficient Ca^{2+} handling and subsequent pathological increase in $[Ca^{2+}]_i$, comprising ischemic injury, glutamate excitotoxicity, epilepsy and trauma (Nishizawa, 2001; Wolf et al., 2001). $[Ca^{2+}]_i$ elevated above 1-3μM overloads mitochondria and leads to $\Delta\psi_m$ depolarization, impaired ATP synthesis, generation of reactive oxygen species (ROS), permeability transition and cell death (Chang and Reynolds, 2006b). Chronic mitochondrial dysfunction found in neurodegenerative diseases is also related to disrupted Ca^{2+} homeostasis in both cells and mitochondria, as has been demonstrated in AD, ALS and HD (Panov et al., 2002; Sheehan et al., 1997; Siklos et al., 1998).

Reactive oxygen species (ROS)

Mitochondria produce ROS for cell signaling, within the normal metabolism of oxygen, and ensure the scavenging of this normally produced ROS by means of enzymes such as superoxide dismutase, catalase and glutathion peroxidase. However, during cellular stress, ROS levels can increase dramatically and contribute to oxidative

damage. If excess damage is caused to mitochondria, cells may undergo apoptosis or programmed cell death.

High-throughput electron transport down the respiratory chain inevitably results in the escape of unpaired electrons, primarily at complexes I and III Reaction of electrons with O_2 yields the highly reactive superoxide anion, which can convert to other ROS such as hydrogen peroxide and hydroxyl radicals. When ROS generation surpasses protective mechanisms of mitochondrial scavenging enzymes, multiple destructive redox reactions may ensue: (1) lipid peroxidation that compromises the integrity of membranes, including mitochondrial membranes, (2) protein oxidation that disrupts enzymes and structural proteins, and (3) oxidative damage to DNA, including mtDNA. ROS are therefore harmful to both cells and mitochondria (Chang and Reynolds, 2006b).

Mitochondrial defects can increase ROS production as well as reduce ROS removal. ROS production is promoted during glutamate excitotoxicity and reperfusion after ischemic injury. In addition, chronic oxidative stress is implicated in many neurodegenerative conditions, including PD, AD, Friedreich's ataxia, ALS and aging (Chang and Reynolds, 2006b; Liu et al., 2002).

Apoptosis

Apoptosis is the prototypical form of programmed cell death that may also occur in a range of neurodegenerative conditions. Apoptosis is characterized by a series of highly regulated biochemical events leading to caspase activation, membrane blebbing, cell shrinkage, changes to the cell membrane such as loss of membrane asymmetry and attachment, nuclear fragmentation, chromatin condensation, and chromosomal DNA fragmentation. Proteins released from mitochondria into the cytosol are important inducers of apoptosis. Cytochrome c is one such protein that forms an apoptosome complex in association with apoptosis protease-activating factor 1, ATP or dATP, and procaspase-9. ATP-dependent activation of procaspase-9 then initiates a proteolytic caspase cascade that leads to cell death. The mitochondrial intermembrane space proteins Smac/DIABLO and Omi/HtrA2, apoptosis inducing factor and endonuclease G are also released and promote apoptosis. Thus, mitochondria harness a cohort of

proteins that can lead to the demise of cells (Chang and Reynolds, 2006b; Crompton, 1999).

The main proapoptotic mechanisms are probably:

- permeabilization of mitochondrial membranes through activation of the mitochondrial permeability transition pore in pathological conditions (Crompton, 1999)

- proapoptotic proteins activating the voltage-dependent anion channel in the outer mitochondrial mebrane (Rostovtseva et al., 2004)

- adenine nucleotide translocator in the inner membrane (Marzo et al., 1998).

5.1.2 Morphology

Mitochondrial morphology is largely diverse (Fig.3). They are reported as filamentous in dendrites or discrete in axons, electrically isolated as well as forming networks. In the course of mitochondrial trafficking, they can elongate, shorten, undergo fission and fusion, thus change the number of independently operating organelles. Mitochondrial fission is defined as the separation of a long tubular mitochondrion (2-5 µm in length) into two or more smaller parts (~0.5 µm in diameter). Mitochondrial fusion stands for the combination of two mitochondria into a single organelle. It occurs at the tips or on the sides of the mitochondria.

These reactions between the outer and inner mitochondrial membrane are modulated by fusion and fission proteins such as mitofusin-1 and dynamin-related protein-1, respectively. Exact mechanism and mediators of fusion/fission behaviour need to be further studied, however there is much speculation about the impact and advantages of different mitochondrial morphologies.

Increasing mitochondrial length and thereby reducing diffusion distance may facilitate proper energy distribution, sequester ions over the given surface area more effectively, and minimize energy loss associated with respiration. On the other hand, fission of mitochondria generates "new" organeles from a given mitochondrial mass. Smaller organelles can respond to different energetic demands in post-mitotic cells and adopt different movement patterns, requiring less ATP to power motility. Moreover, discrete mitochondria are protected from mitochondrial damage or depolarization, which would spread through extensive mitochondrial network, implying that injury-

induced mitochondrial division may be a protective mechanism (Chang and Reynolds, 2006b).
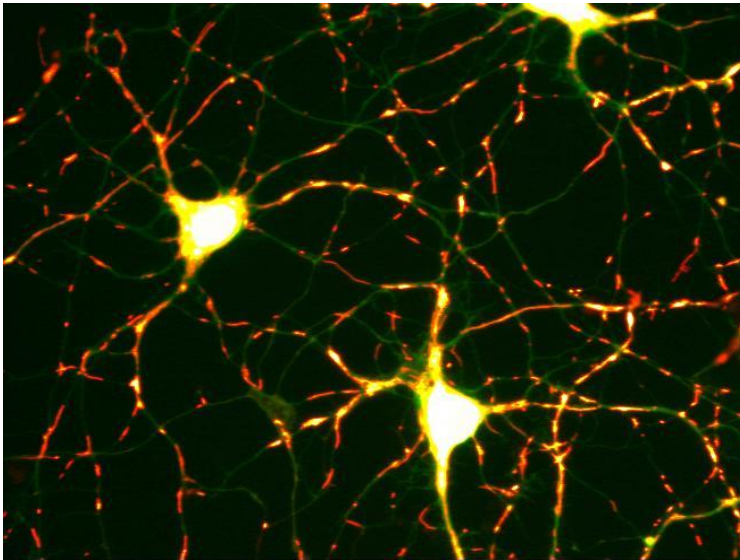
Figure 3 Mitochondrial distribution in neuronal processes. Representative imposed image of cortical neurons processes (green fluorescence) and associated mitochondria (in red) from our experiment. Mitochondrial morphology varies from small rounded to elongated filamentous particles.

Aside from being protective, mitochondria remodeling, particularly shortening, swelling and fragmentation, is considered to be consequence of mitochondrial exposure to neurotoxins such as zinc, mobilized during ischemic brain injury, or to glutamate activating N-methyl-D-aspartate (NMDA) receptors (Reynolds et al., 2004). It has been proposed that fission of mitochondria is associated with apoptotic cell injury, thus making an important contribution to the fate of the cell (Chang and Reynolds, 2006b; Frank et al., 2001).

5.1.3 Movement

Mitochondria are highly dynamic organelles that fuse, divide, move and replicate, exhibiting a finite lifetime that is typically shorter than the life of the host cell.

Balanced mitochondrial movement regulates cell health and homeostasis as well as disposal of damaged mitochondria for degradation by autophagy.

In neurons, mitochondrial distribution is uniform, generated by local regulation of the stopping events of fast mitochondrial transport (Miller and Sheetz, 2004). Over half of the mitochondria are stationary, whereas the rest move at velocities of 0.3–2.0 µm/second in each direction. The means and distributions of the velocities are similar (Ligon and Steward, 2000).

It has been demonstrated that mitochondrial movement increases during synaptic activity, making synapses targets for long-term mitochondrial localization and dynamic recruitment of moving mitochondria in spontaneously firing neurons (Chang and Reynolds, 2006b).

Mechanism of movement

Three major protein groups are involved in transporting mitochondria in neurons: cytoskeletal proteins, molecular motors, adaptor and scaffolding proteins that mediate interactions between motors, cargos and the cytoskeleton (Fig. 4). Several proteins outside of these classes have also been implicated as modulators of movement.

Motor activity and association with cargo are regulated by conformational changes, de/phosphorylation, abundances of motor proteins and different microtubule associated proteins (Reilein et al., 2001; Sheetz, 1999). Interestingly, motor proteins on mitochondria are distributed in discrete clusters that seem to generate force independently of each other, suggesting that differential regulation of individual motor protein clusters may mediate changes in velocity and direction (Chang and Reynolds, 2006b).

Mechanisms of mitochondrial docking are thought to be based on the structure and length of cytoskeletal filaments or affected by nerve growth factor (NGF) chemoattraction (Lee and Peng, 2006).
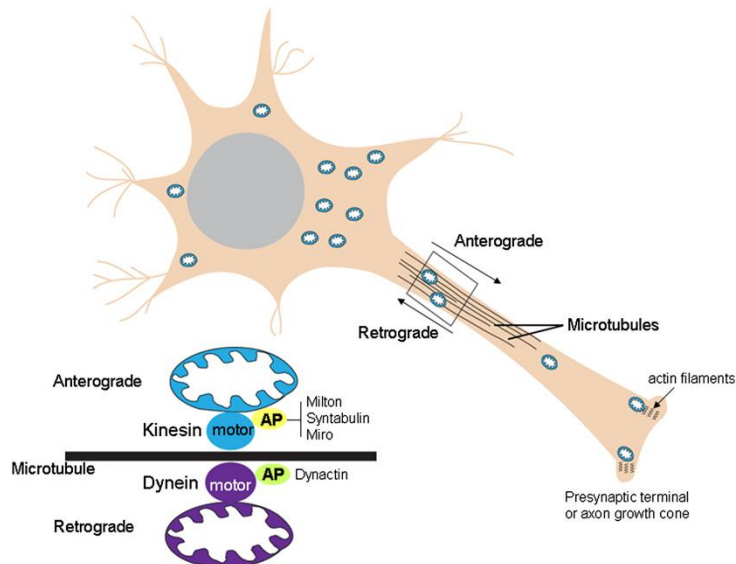
Figure 4. Mitochondrial trafficking mechanisms within the axon. Mitochondria move along microtubule tracks either toward the presynaptic terminal (anterograde transport), which is ensured by ATP-dependent motor proteins kinesins, or toward the cell body (retrograde transport) due to dynein motor proteins. Mitochondria associate with the motor proteins through specific adaptor proteins (AP). AP for kinesins include Milton, syntabulin, and a Rho GTPase called Miro. Dynactin is an AP for dynein. Mitochondria can also move along actin filaments by a myosin-mediated mechanism, as it was described in the axonal growth cone and presynaptic terminal (Adapted from Mattson et al., 2008).

Patterns of motility

It has been suggested that at least three populations of mitochondria may exist with different motility characteristics and functional capacities. They are (1) relatively stationary mitochondria, docked at nonsynaptic sites for > 15 min, (2) mobile mitochondria that pause on the order of seconds and (3) mobile mitochondria that pause on the order of minutes (Chang and Reynolds, 2006b).

Trushina et al. (2004) recorded mitochondria in mammals and distinguished more detailed patterns of motion. In addition to stationary mitochondria , which did not move during the time of experiment, mitochondria were considered to move smoothly if they did not stop over the distance of 50μm (the average length of the neurite in experiments was about 60 μm). Mitochondria that moved back and forth without net displacement were scored as saltatory. Many mitochondria underwent stop-and-go motion where they moved, stopped, and then resumed movement often changing the direction. Thus, mitochondrial movement patterns are highly variable between axons

and dendrites, but also in different types of neurons at different developmental stages (Chang and Reynolds, 2006b).

Young/mature neurons

Neurons develop from undifferentiated neuroblasts that lack any sort of axonal or dendritic specialization. Therefore, mitochondria are initially located in the cell soma. When neuronal processes sprout and elongate, an axon is designated, axonal and dendritic branches form and remodel, and synaptic connections assemble and mature, so that neuron have an intense need for ATP. Mitochondria localize to active growth cones by chemoattraction to NGF and become increasingly important as development proceeds (Chang and Reynolds, 2006b).

Chang and Reynolds (2006a) demonstrated that in younger cortical neurons mitochondria were more mobile, shorter, occupied a smaller percentage of neuronal processes, and expressed greater mitofusin-1 and lower dynamin-related protein-1 protein levels than in older cortical neurons. However, the number of mitochondria per μm of neuronal process, mitochondrial membrane potential and the amount of basally sequestered mitochondrial Ca^{2+} were similar. While mitochondria in young neurons are functionally similar to mature neurons, their enhanced motility may permit faster energy dispersal for cellular demands, such as synaptogenesis. As cells mature, mitochondria in the processes may then elongate and reduce their motility for long-term support of synaptic structures.

Axon/dendrite

The transport of mitochondria in axons and dendrites is similar despite any cytoskeletal or differences in demand between the two domains. Nevertheless, some studies state that mitochondria in axons tend to travel farther and with consistently rapid velocity than those in dendrites. High synaptic density in dendrites correlates with reduced mitochondrial movement and longer morphology compared to axons (Chang and Reynolds, 2006b; Ligon and Steward, 2000).

Antero/retrograde

Anterograde transport is defined as movement from the cell body to the synapse

19

and comprise approximately 70% of all mitochondrial movement (Ligon and Steward, 2000), whereas retrograde movement is directed from the axon back to the cell body. 90% of mitochondria with high membrane potentials move anterogradely toward growth cones and approximately 80% of mitochondria with low potential are transported towards the cell body, however the reason for bidirectional transport of mitochondria is still uncertain.

It is hypothesized that healthy mitochondria, synthesized in the cell bodies of neurons, are distributed by anterograde transport down the axon to accomplish their function. During aging, mitochondria become heterogeneous in potential and on average become more depolarized, they return to the cell body for repair or recycling in an acidic lysosomal compartment by autophagy (Miller and Sheetz, 2004). In spite of that, there is still no evidence excluding mitochondrial autophagy in neuronal processes (Chang and Reynolds, 2006b). Mean mitochondrial speeds are reported to be similar in the anterograde and retrograde direction, but while the probability of moving in either direction is equal in axons, it is increased in the anterograde direction in dendrites (Chang and Reynolds, 2006b; Ligon and Steward, 2000)

5.1.4 Movement abnormalities

Trafficking is intimately tied with the functional status of cells and of the organelles themselves, they move over extreme distances to maintain cellular homeostasis in very large and active cells such as neurons, thus normal mitochondrial dynamics are crucial for neuronal health. Trafficking impairment may have different origins and contribute to various patterns of neurodegeneration and neuronal death (Fig.5).

The time over which mitochondrial movement is impaired, recovers or if it is followed by concurrent cellular and mitochondrial defects, affects the course of neuronal dysfunction and death. Neurotoxicity could be acute, if mitochondria stopped moving abruptly, as in the case of glutamate excitotoxicity, or delayed if mitochondria stopped moving gradually, as expected in neurodegenerative diseases (Chang and Reynolds, 2006b, Trushina et al., 2004).
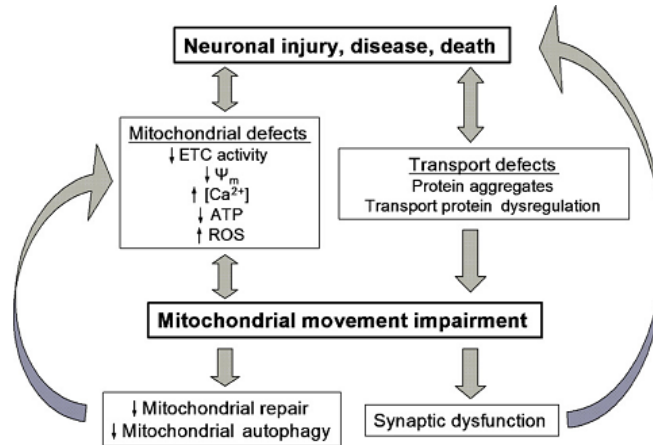
Fig.5 Relationship between impaired mitochondrial movement, mitochondrial dysfunction and neuronal injury and disease (Adapted from Chang and Reynolds, 2006b).

Prolonged impairment of mitochondrial movement may also inhibit fusion-mediated mtDNA complementation and autophagic degradation of damaged mitochondria (Ono et al., 2001; Priault et al., 2005). As a result, mtDNA mutations can accumulate and cause electron transport defects and ROS production that leads to further mtDNA mutation, lipid peroxidation, protein oxidation, and ultimately cell death (Andersen, 2004).

Chronic movement disruption

Disrupted trafficking of all mitochondria in chronically diseased neurons may very well be caused by mitochondrial dysfunction, since common features of AD, ALS and HD are $\Delta\psi_m$ depolarization, respiratory defects and abnormal $[Ca^{2+}]_i$ homeostasis. However, it is discussed to be imposed by interactions between abnormal proteins and cytoskeletal or motor protein constituents as well. For instance, protein aggregation and accumulation seems to be a common manifestation in almost all polyQ diseases and AD. Such accumulation of misfolded proteins is perhaps a major trigger of cellular stress and neuronal death. Aggregates impair the passage of mitochondria along neuronal processes by acting as roadblocks, or by associating directly with mitochondria, causing their accumulation and immobilization in the vicinity of aggregates. Furthermore, mitochondrial trafficking is reduced specifically at sites of

aggregates (Anandatheerthavarada et al., 2003; Chang et al., 2006, Gunawardena and Goldstein, 2001; Trushina et al., 2004).

Recent studies have identified an altered microtubule-dependent transport of organelles in AD, ALS, HD, PD, spinobulbar muscular atrophy, dentatorubral-pallidoluysian atrophy or spinocerebellar ataxias. Neurons contacting the diseased cells degenerate, probably with postsynaptic neurons degenerating before presynaptic neurons in correspondence with the earlier axonal degeneration of the injured neurons. (Chang and Reynolds, 2006b; Gunawardena and Goldstein, 2001; Miller and Sheetz, 2004; Szebenyi et al., 2003; Trushina et al., 2004).

Therefore, drugs restoring the function of microtubules and consequently improving mitochondrial trafficking, are expected to be a promising treatment for many presently cureless neurodegenerative diseases.

5.2 Histone Deacetylases

HDAC (EC number 3.5.1) are a class of enzymes that remove acetyl groups from an ε-N-acetyl lysine amino acid on a histone and other important cellular proteins. They have been recognized as potentially useful therapeutical targets of various human disorders, primarily cancer and currently also neurodegenerative diseases.

5.2.1 Mechanism of activity

The steady-state levels of histone acetylation depends on the activity of histone acetylases (HATs) and HDACs, multiprotein complexes which act as coactivator or corepressor, respectively (Sun et al., 2003). (Fig. 6.)
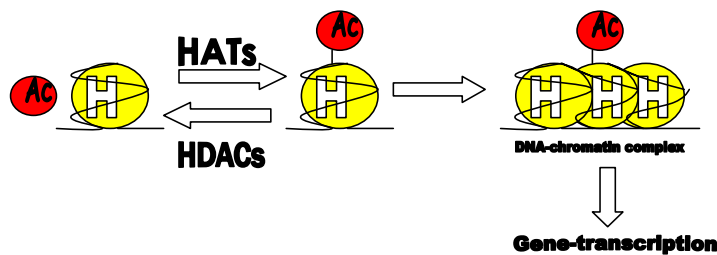
Figure 6 Mechanism of HDAC activity. Histone (H) acetylation is mediated by histone acetylases (HATs). Acetyl groups (Ac) are attached on specific amino acids, usually lysines. Conformational structure of DNA-chromatin complexes is established subsequently to acetylation of histones and transcriptional gene expression is triggered. Histone deacetylases (HDACs) cause transcriptional repression by converting the chromatin structure into the condensed form that is not transcripted.

In general, increased histone acetylation evokes remodelling of chromatin from tightly packed configuration to a loosely packed configuration, which consequently activates transcription. Conversely, a decrease in histone acetylation may cause a condensation of chromatin structure and leads to transcriptional silencing. Thus, upregulation of transcription can be achieved either by stimulation of HAT or by inhibition of HDAC activities, and the opposite for transcriptional downregulation (Kazantsev and Thompson, 2008).

In addition to modification of histones, other cellular proteins are substrates for HDACs, and these proteins mediate diverse biological functions via transcriptional-dependent as well as independent mechanisms, which were probably the primary HDACs activity because three HDAC classes preceded the evolution of histone proteins (Gregoretti et al., 2004; Zhang et al., 2003). Protein acetylation is post-translational modification that regulates numerous cellular functions, including metabolism, ageing, inflammation, microtubule dynamics and intracellular transport (Kazantsev and Thompson, 2008).

5.2.2 HDAC superfamily

Since the identification of the first histone deacetylase (Taunton et al., 1996), 18 new members have been identified in humans, but few have been characterized in detail. The superfamily of HDAC can be divided into four equally distinct groups: classes I, IIa and IIb, the structurally different class IV, and unrelated III sirtuin deacetylases (Gregoretti et al., 2004). (Fig.7)

The name HDAC has historic origin, however, histones are not enzymatic substrates for some deacetylases in a given family, and are not exclusive substrates for other family members (Kazantsev and Thompson, 2008).
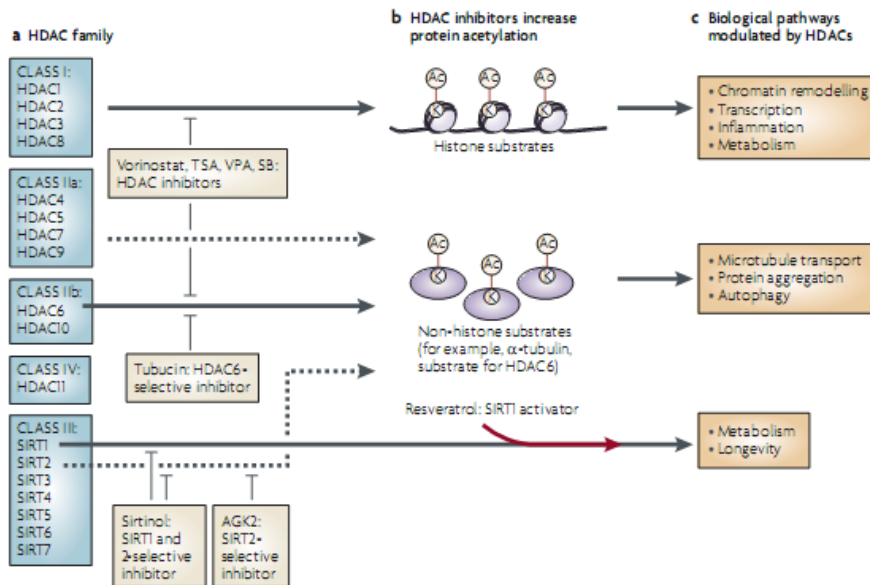
Fig. 7 Therapeutic targeting CNS diseases with small-molecule inhibitors.
a) HDAC family (classes I–IV) and HDACs implicated as disease modifiers. b) Shown to be efficacious in animal disease models the HDAC inhibitors vorinostat (also known as SAHA), trichostatin A (TSA), valproic acid (VPA) and sodium butyrate (SB) upregulate histone and α-tubulin acetylation in cellular assays. The roles of other specific HDAC isoforms in modulating disease pathology are yet to be determined with assistance of isoform-selective and class-selective inhibitors. Selective upregulation of α-tubulin acetylation in cellular assays is shown for the HDAC6-specific inhibitor tubucin as an example. c) Disease-modifying pathways, which underlie mechanisms implicated in HDAC inhibitor efficacy (Adapted from Kazantsev and Thompson, 2008).

Class I HDACs

Class I and class II HDACs include the Zn^{2+} -dependent deacetylases, which share significant structural homology. Class I contains the ubiquitously expressed HDAC1, HDAC2 and HDAC3, and the muscle-specific HDAC8. HDAC1 and HDAC2 are predominantly localized in the nucleus, whereas HDAC3 is able to shuttle between the nucleus and cytoplasm. Class I enzymes are expressed in the CNS, as well as in peripheral tissues, thus they may have a broad role in controlling histone acetylation and transcription.

Class II HDACs

Class IIa HDACs includes four members – HDAC4, HDAC5, HDAC7 and HDAC9 – with distinct specific patterns of expression, predominantly in muscle and

heart. HDAC9 is localized in the nucleus, while its catalytic domain lacking variant MITR shuttle between the nucleus and cytoplasm as well as other class IIa members.

Only two enzymes – HDAC6 and HDAC10 belong to class IIb. The structure of HDAC6 is unusual in that it contains two independently functioning catalytic domains and a carboxy-terminal Zn^{2+} -finger ubiquitin binding domain. HDAC6 deacetylases α-tubulin and alters microtubule stability. Acting in the cytoplasm, HDAC6 regulates microtubule-dependent transport and cytoskleton dynamics. HDAC6 is expressed in most neurons but is most abundant in cerebellar Purkinje cells, large cerebellar neurons vulnerable to degeneration by spinocerebellar ataxia (Hahnen et al., 2008; Kazantsev and Thompson, 2008). Regulation of protein degradation by HDAC6-dependent retrograde transport on microtubules is another important function for maintenance of cellular homeostasis in the brain (Iwata et al., 2005), moreover it regulates the activity of chaperon heat shock protein 90, which provide another insight into the role of this deacetylase by protein degradation (Kazantsev and Thompson, 2008).

HDAC10 is a close structural homologue of HDAC6 with unknown exact functions, however as several other class II HDACs, it has been shown to interact with class I HDAC3 indicating a tight functional connection between class I and II isoenzymes (Kazantsev and Thompson, 2008).

Class IV HDACs

HDAC11, unique member of class IV, is predominantly localized in the nucleus, however it may be present in protein complexes that also contain cytosolic HDAC6. Its function is poorly understood, though HDAC11 has presumably distinct physiological roles from those of the known HDACs (Gao et al., 2002).

Class III HDACs

By contrast, the class III deacetylases, or sirtuins, are structurally and functionally different from other HDACs. Their name derived from the first sirtuin identified in budding yeast - the silent information regulator 2 (Sir2) gene. Sirtuins are different in their absolute dependence on NAD^+ to carry out catalytic reactions. This class contains seven members with multiple functions. Neuroprotective effect shows SIRT1 activation as well, either genetically or pharmacologically, or via metabolic

conditioning associated with calorie restriction. An increase of SIRT1 activity could enhance transcriptional expression of neuronal anti-stress, anti-apoptotic and anti-inflammatory genes. SIRT1 is highly expressed in the brain, spinal cord and dorsal root ganglia during embryonic development, which suggest an involvement of this deacetylase in neurogenesis (Kazantsev and Thompson, 2008; Li et al., 2007).

Interestingly, SIRT2 is a cytosolic protein that deacetylates α-tubulin and microtubules, as well as HDAC6, and provides neuroprotective benefit in neurodegeneration models, however it can be localized also in nucleus. In addition, some sirtuins have been identified in mitochondria (SIRT3, SIRT5), their function is not yet known but they are supposedly implicated in the regulation of cellular metabolism and ageing like other sirtuins (Kazantsev and Thompson, 2008; North et al., 2003).

5.3 Histone deacetylase inhibitors (HDACi) in the CNS

HDACi have a long history of use, for instance in psychiatry and neurology as mood stabilizers and antiepileptic compounds (including VPA). During the past six years, numerous studies identified these small-molecule HDAC ligands as candidate drugs for the treatment of neurodegenerative disorders, and clinical trials have been initiated to evaluate the safety and efficacy of HDAC inhibitors (Hahnen et al., 2008).

5.3.1 Mechanism of activity

HDACi counteract HDAC enzymes, thus increasing acetylation of histones and other target proteins (Fig.8), and affecting various cellular functions. They may restore transcriptional balance to neurons, modulate cytoskeletal function, affect immune responses and enhance protein degradation pathways (Kazantsev and Thompson, 2006).
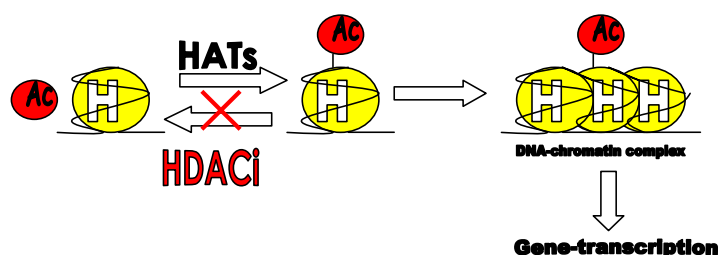
Figure 8 Effect of HDAC inhibitors on chromatin remodelling and transcription. HDAC inhibitors (HDACi) block the deacetylation counteracting HDAC enzymes, thus they change the equilibrium of histone (H) acetylation (Ac) levels. Consequently to increased acetylation, chromatin is relaxed and transcription is upregulated.

Transcriptome wide studies have demonstrated that HDACi can affect the transcription levels of 7-10% of all genes (Xu et al, 2007). These changes are not based only on histone hyperacetylation, numerous non-histone protein targets of HDACs including transcription factors and regulators, signal transduction mediators, DNA repair enzymes, nuclear import regulators, chaperone proteins, structural proteins, inflammation mediators and viral proteins are likely to contribute to the reported effects induced by HDACi.

Furthermore, there is the finding that HDAC inhibitors (TSA) antagonize gene silencing by DNA methylation mediated by methyl-CpGbinding protein 2. In vivo

experiments show that TSA, VPA, essential HDACi members, and SNDX-275 trigger DNA-demethylation in a replication-independent manner. These results suggest that apart from hyperacetylation, HDACi may alleviate DNA-methylation, although the exact mechanism by which HDAC inhibitors affect DNA methylation remains to be clarified (Hahnen et al., 2008).

5.3.2 Characterization of HDACi

Small molecule HDACi investigated for the potential treatment of neurodegenerative disorders primarily affect class I and II HDAC, not class III (sirtuin) activities. They differ in potency and HDAC isoenzyme selectivity and grouped into four different classes: (1) short chain fatty acids, (2) hydroxamic acids, (3) benzamides, and (4) cyclic tetrapeptides.

Short chain fatty acids

This group includes sodium butyrate (SB), phenylbutyrate (PB) and valproic acid (VPA). SB was suggested to have HDAC inhibitory function in 1977, linked to previously reported antiproliferative effects. PB, and SB derivative, is currently an orphan drug which achieved FDA approval for the treatment of urea cycle disorders. VPA is a commonly used anticonvulsant and mood stabilizator, approved by FDA in 1987, currently in several clinical trials as HDACi (see below).

Hydroxamic acids

TSA and vorinostat (also known as SAHA and Zolinza) are prime members of hydroxamic acid group of HDACi. Both are pan-HDACi like several other hydroxamic acids (e.g. scriptaid, oxamflatin, carboxycinnamic acid bishydroxamic acid and suberic bishydroxamic acid), apparently without profound HDAC isoenzyme selectivities.

Benzamides and cyclic tetrapeptides

The Benzamide-based HDACi group contains primarily compounds 106 and HDAC1 selective MS-275 (SNDX-275). The cyclic tetrapeptide romidepsin (FK-228, depsipeptide) is active at low nanomolar doses and shows little activity against HDAC6 while the cyclic tetrapeptide apicidin appears to be highly selective with a pronounced

activity against class I HDAC2, HDAC3 and HDAC8 (Hahnen et al., 2008; Khan et al., 2008). Interestingly, a microbially derived tetracyclopeptide trapoxin was the first demonstrated compound that inhibited histone deacetylation in vivo and caused mammalian cells to arrest in the cell cycle, acting as key regulator of eukaryotic transcription (Taunton et al., 1996).

Sirtuin ligands

Among sirtuin ligands, there are activators such as SRT1720 and resveratrol, or inhibitors represented by sirtinol and AGK2. Animal efficacy of the putative SIRT1 activator resveratrol was assessed and demonstrated in various disease models, however there may be low bioavailibility in mammals, low solubility and sensitivity to oxidation according to its structure (Kazantsev and Thompson, 2008).

In summary, with respect to the potential treatment of neurodegenerative conditions, investigation of HDACi is mainly focused on the well-established experimental drug TSA and the clinically used HDACi, namely, SB, PB, VPA and SAHA, which are all known to penetrate the blood – brain barrier (Hahnen et al., 2008). Nevertheless, a recent focus of intensive investigation has been to develop class-specific and isoform-specific HDACi to avoid undesirable epigenetic changes by inhibition unintentional enzymes, beside specific inhibitors may also be less toxic than pan-HDACi.

Selective HDACi

Notwithstanding evolutionary conserved architecture of the HDAC active site, class I-selective HDACi have been reported. Pan-HDACi upregulated both acetylation of histones and α-tubulin, whereas inhibitors selective for class I enzymes increase only histone acetylation. However the effects in cells of class I-selective inhibitors on other class complexes and activities are yet to be examined.

Using a functional test for class IIb HDAC6 inhibition, induced hyperacetylation of α-tubulin, MC1568 was described as a class II selective inhibitor, applied for HDAC6 and HDAC4 inhibition (Kazantsev and Thompson, 2008). A multidimensional, chemical genetic screen was used to discover tubacin, which is selective HDAC6

inhibitor in mammalian cells. Domain selective tubacin does not affect the level of histone acetylation, gene-expression patterns, or cell-cycle progression, but inhibits α-tubulin deacetylation and decrease cell motility (Haggarty et al., 2003).

5.3.3 Pharmacological properties

HDACi for CNS disorders treatment need to be stable and bioavailable compounds to penetrate the blood-brain barrier and reach affected brain tissues. Inhibitors are both potent and selective for specific intracellular molecular targets, and isoform-specificity or at least class-specificity is desired to minimize nonspecific side effects. In addition, several challenges are associated with development of drugs exhibiting less cytotoxicity. The first identified pan-HDACi derived from hydroxamic acids are currently in clinical development, though nonspecific cytotoxicity as well as low isoform selectivity may contibute to their setback. On the other hand, benzamide head group exhibits less toxicity properties and greater brain permeability, which is a further major limitation for effective drug treatment.(Kazantsev and Thompson, 2008).

5.3.4 TSA

Trichostatin A (Fig.9) is a prominent member of hydroxamate-based HDACi. It was isolated from the metabolites of strains of *Streptomyces hygroscopicus* in 1976 to serve as antifungal antibiotic (Tsuji et al., 1976).

Figure 9 Structure of TSA.

In 1990, Yoshida et al. demonstrated that TSA is a potent and specific inhibitor of the histone deacetylases class I and II and that the in vivo effect of TSA on cell proliferation and differentiation can be attributed to the inhibition of these enzymes.

TSA is one of the highly potent pan-HDAC inhibitors active already at low nanomolar doses (IC_{50}: 12 nM) (Miller et al., 2003). For example, deacetylase activities of purified HDAC1 and HDAC3 were potently inhibited by TSA detecting IC_{50} at 1.5nM (HDAC1) and 0.6nM (HDAC3). Such potency of this small molecule has been attributed to the ability of the inhibitor functional groups to access the zinc cation in the HDAC active-site pocket. TSA coordinate the zinc in a bidentate manner and simultaneously contacts residues that are likely to be involved in catalysis by its hydroxamate active half. This interaction efficiently inactivates the zinc-dependent deacetylase activity of HDAC (Kazantsev and Thompson, 2008).

Its high potency makes TSA a well-established experimental drug, with future promising use in alleviating of neurodegenerative disorders. For instance, TSA manifests an ameliorating effect on the SMA disease phenotype in vivo mouse models (Avila et al., 2007). Also, Kanai et al. (2004) found that HDACi including TSA, VPA (at therapeutic concentrations used for the treatment of bipolar mood disorder and seizures) and SB, robustly protected mature cerebellar granule cell cultures from activated NMDA-receptor excitotoxicity, in correlation with increased acetylated histones levels.

5.3.5 VPA

Valproic acid (Fig.10) has short fatty acids structure and penetrates the blood-brain barrier. It achieved FDA approval as neuroleptic drug in 1987 (Hahnen et al., 2008).

VPA is also known to be a potent teratogen in humans and rodent animal models. Structural and functional studies of VPA and related compounds suggest that the teratogenic and anticonvulsant effects of VPA can be separated and therefore may be mediated by distinct mechanisms (Kanai et al., 2004).

Figure 10 Formula of VPA.

VPA´s HDAC inhibitory function was discovered in 2001. VPA inhibits total HDAC activity incompletely, being reported as selective class I inhibitor. It acts in the milimolar range of concentrations (IC_{50} for HDAC1=0.4 mM), being less potent than TSA ,however submillimolar doses of VPA in single cell cultures were also effective in altering histone acetylation levels. Moreover, VPA reduces HDAC2 (class I) protein levels by proteosomal degradation of HDAC2 but not of other class I HDAC isoenzymes (Hahnen et al., 2008; Phiel et al., 2001).

Emerging evidence suggests that VPA is neuroprotective, by inhibiting some forms of apoptosis, protecting against endoplasmic reticulum stress in C6 glioma cells, or by inducing axonal remodelling and synapsin clustering, presumably through indirect inhibition of glycogen synthase kinase-3 (Kanai et al., 2004). Additionally, VPA induces proneuronal factors in association with histone acetylation and in consequence promotes neuronal differentiation (Yu et al., 2009).

5.3.6 Possible therapeutical use of HDACi in neurodegenerative disorders

Ongoing clinical trials for the potential treatment of HD, amyotrophic lateral sclerosis (ALS) and spinal muscular atrophy (SMA) are focussed on PB and VPA, which are well-tolerated drugs and likely suitable for long-term treatment but weak HDAC inhibitors in comparison to TSA. In animal trials, high drug concentrations have been applied, ranging from 250 to 530 mg/kg for VPA and 100 to 1200 mg/kg for SB and PB. These drugs are neuroprotective, however it is uncertain if such effective concentrations are achievable in the patient's central nervous system. Therefore, the aim

33

of future studies and trials will address the therapeutical use of highly potent HDACi including TSA or SAHA, further decoding the HDAC selectivity of known inhibitors, and developing more selective HDACi (Hahnen et al., 2008).

Potential areas for therapeutic interventions are:

5.3.6.1 Polyglutamine disorders

Polyglutamine (polyQ) expansion diseases are a class of nine inherited neurodegenerative disorders that are known to be caused by mutations in polyglutamine-encoding CAG tracts in different genes that result in degeneration of different populations of neurons. This group contains HD, Dentatorubral-Pallidoluysian atrophy, spinal and bulbar muscular atrophy (SBMA, Kennedy disease) and six spinocerebellar ataxias (types 1, 2, 3 – Machado Joseph disease, 6, 7 and 17). All referenced disorders are caused by expansions of polymorphic $(CAG)_n$ repeats in the coding regions of the disease genes leading to long polyQ stretches, which confer a gain-of-function to the mutant proteins. They have many features in common and thus might be treatable by common pharmacologic interventions.

HD is caused by neuronal dysfunction and progressive neuronal cell death that is especially severe in the striatum. The disease is characterized by choreic movements, neuropsychiatric symptoms and severe cognitive deficits. The polyQ expansion (the CAG repeat number is expanded to > 40 and unstable in HD patients) in the mutant huntingtin protein (htt) leads to its aberrant proteolytic cleavage, resulting in the release of N-terminal fragments form aggregates in brain tissue from affected patients (Hahnen et al., 2008).

It has been recently demonstrated in HD patients that a microtubule-dependent transport of organelles is altered and contributes to the neuronal toxicity. HD brains reveal reduced tubulin acetylation which can be compensated by HDACi targeting HDAC6 (Dompierre et al., 2007; Guanawardena and Goldstein, 2001; Trushina et al., 2004). Additional studies provide strong evidence for transcriptional dysregulation as a mechanism of HD pathogenesis showing that mutant huntingtin expression leads to a change in HAT activity, or impairs the function of several nuclear proteins involved in

the transcription machinery which can be partly compensated by treatment with (Hahnen et al., 2008; Sadri-Vakili and Cha, 2006).

Currently, there is no treatment available for HD patients, although starting with yeast studies, Drosophila, Caenorhabditis elegans and R6/2 and other mice with polyQ expansion models for HD, members of HDACi have been identified as compounds of therapeutic interest. A neuroprotective effect by correcting global histone hypoacetylation induced by mutant htt and ameliorating the HD phenotype in vivo has been shown for TSA, SAHA and SB. These drugs are not specific for a given HDAC and affect histones as well as other proteins including microtubules. Based on these findings a clinical Phase II trial has been initiated to assess the safety and tolerability of PB for potential HD treatment. Additionally, a pilot trial using VPA for the adjuvant therapy of HD patients revealed improved motor scores (Dompierre et al., 2007; Hahnen et al., 2008).

Although DRPLA, SBMA and spinocerebellar ataxias affect neurons of other regions, mouse models experiments indicate histone hypoacetylation and therefore possible treatment with HDACi (SB, TSA, SAHA) as in HD, even after disease onset (Kazantsev and Thompson, 2008).

5.3.6.2 Motor-neuron diseases

The motor-neuron diseases include spinal and bulbar muscular atrophy (SBMA), the inherited spinal muscular atrophy (SMA) and amyotrophic lateral sclerosis (ALS).

SMA is caused by an absence of the survival motor neuron (SMN) 1 gene, while SMN2 gene copies affect the disease severity. VPA is currently in clinical trials for the SMA treating, however SAHA or romidepsin inhibited levels of HDAC2 preventing harmful consequences of survival motor neuron genes mutation, more potently. These two HDACi bypass SMN2 gene silencing by DNA methylation (Hauke et al., 2009).

TSA improved animal survival and protection of motor neurons when administered after disease onset, also activating SMN gene expression. PB and sodium valproate promoted motor-neuron survival in mouse models of ALS through amelioration of abnormal histone hypoacetylation and transcriptional dysregulation, which is implicated in ALS. SBMA's phenotypic symptoms, triggered by a polyQ

expansion within the androgen receptor, are ameliorated by SB which increases histone acetylation in SBMA (Kazantsev and Thompson, 2008).

5.3.6.3 Antinflammatory effects

Stroke, a cerebral ischemia, is another target for HDACi treatment. Recent studies use a rat middle cerebral artery occlusion model of stroke to show the multiple effects of HDACi on ischemia-induced brain infarction, neuroinflammation, gene expression, and neurological deficits (Hahnen et al., 2008; Kazantsev and Thompson, 2008).

It has been found that post-occlusion injections with HDACi (VPA, SB, TSA) decreased brain infarct volume. Post-insult treatment with VPA or SB also suppressed microglial activation, reduced the number of microglia, and inhibited other inflammatory markers in the ischemic brain. HDACi treatment prevented the ischemic brain reduction in levels of acetylated histone H3. Moreover, it seems that HDACi also superinduced heat-shock protein 70, inhibit both activation of some pro-apoptotic pathways (p53, phospho-Akt), and induction of nitric oxide synthase and cyclooxygenase 2. Therefore, potential use of HDACi for clinical trials in stroke patients are presently expected (Kim et al., 2007b).

Another disease involving inflammation and neuronal apoptosis is multiple sclerosis. TSA, the histone deacetylase inhibitor, reduces spinal cord inflammation, demyelination, neuronal and axonal loss and ameliorates disability in the relapsing phase of experimental autoimmune encephalomyelitis, a model of multiple sclerosis. TSA improves a transcriptional inbalance that may contribute to immune dysregulation and neurodegeneration in multiple sclerosis (Camelo et al., 2005).

5.3.6.4 Metabolism and ageing

Impaired lipid metabolism is a risk factor of many neurodegenerative diseases, such as Alzheimer or Niemann-Pick type C (NPC) disease, a neurodegenerative and lipid storage disorder for which no effective treatment is available. It has been reported that VPA enhances neuronal differentiation and restores defective cholesterol traffic in neural stem cells derived from NPC mice (Kim et al., 2007a). Moreover, recent data introduce the class III HDAC (SIRT1) as a potential modulator of cholesterol biosynthesis through liver X receptor, affecting atherosclerosis and other aging-

associated diseases (Li et al., 2007). Furthermore, impaired cholesterol biosynthetic pathways have been identified as a progressive and early marker of Huntington's disease pathogenesis in several mouse models of the disease. In cultured neurons expressing mutant huntingtin and in the brains of mutant huntingtin-expressing animals, accumulated cholesterol was found with evidence for disrupted caveolin-1-mediated cellular trafficking. The use of HDACi may be useful in restoring cholesterol biosynthesis and transport, and may help to elucidate the mechanism involved with cholesterol homeostasis (Kazantsev and Thompson, 2008).

5.3.6.5 Other possible indications

Adrenoleukodystrophy

X-linked adrenoleukodystrophy (X-ALD) is an inherited disease, characterized by pathologic accumulation of very long chain fatty acids in all tissues of the body, progressive demyelination of the central nervous system and adrenal insufficiency. β-oxidation of fatty acids is impaired due to mutation in the ABCD1 gene which encodes the adrenoleukodystrophy protein. Deficiency of this protein could be compensated by ABCD2 gene, whose regulation is a promising target for HDACi. However, other mechanisms of increased β-oxidation by TSA or PB-treatment may be of relevance (Hahnen et al., 2008).

Alzheimer's disease

Alzheimer's disease (AD) is the most common form of dementia in elderly and therapies that prevent or delay its onset are urgently needed. It is characterized by the neuropathological findings of intracellular neurofibrillary tau aggregation and extracellular amyloid plaques accumulating in vulnerable brain regions. Several studies revealed also an accumulation of the protein fragment p25 in sporadic AD.

Recovery of learning and memory impairments, the signature features of AD, is associated with chromatin remodelling and it can be mitigated by HDACi (SB, TSA). Exploratory activity of experimental mice (promoted by the presence of toys, tunnels and climbing devices in the large cages) induced histone H3/H4 hyperacetylation in wild-type mice and normalized memory performance in diseased CK-p25 mice (Hahnen et al., 2008).

It has also been demonstrated that nicotinamide, a competitive inhibitor of the sirtuins HDACs in AD mice, restores cognitive deficits associated with pathology by increased acetylation of α-tubulin, a primary substrate of SIRT2 which is linked to increased microtubule stability. Additionaly, nicotinamid selectively reduces a specific phospho-species of tau that is associated with microtubule depolymerization, in a manner similar to inhibition of SIRT1 (Green et al., 2008).

Fragile X syndrome

The leading cause of inherited mental retardation, Fragile X syndrome (FXS), is due to a CGG sequence methylation and expansion in the FMR1 gene, which results in its silencing. Local hypermethylation and gene silencing is also associated with chromatin remodeling, which can be ameliorated by TSA treatment in *Xenopus laevis* oocytes. Furthermore, it has been shown in a cell-based model that a reactivation of FMR1 gene can be achieved by the DNA demethylating drug 5-azadeoxycytidine, and, to a lesser extent, with the histone deacetylating drugs PB, SB or TSA (Kazantsev and Thompson, 2008).

Novel experiments confirmed the histone hyperacetylation effect of VPA but do not support its putative role in DNA demethylation. Therefore, the combination of 5-azadeoxycytidine with either HDACi in combinatorial therapy, leading to a robust transcriptional reactivation, suggests a possible approach for the treatment of human CNS diseases (Tabolacci et al., 2008).

An alternative strategy to reactivate FMR1 expression or simply another ingredient to "FXS drug coctail" is the pharmacological inhibition of SIRT1. This class III HDAC inhibition also increases histone acetylation levels and shows much larger effects on gene reactivation than other HDACi. Since DNA methylation inhibitors (5-azadeoxycytidine) require DNA replication in order to be effective, SIRT1 inhibitors may be more useful for FMR1 gene reactivation in post-mitotic cells like neurons where the effect of the gene silencing is most obvious (Biacsi et al., 2008).

Friedreich's ataxia

Friedreich's ataxia is an autosomal recessive neurodegenerative and cardiac disease, caused by abnormally low levels of frataxin, an essential mitochondrial protein.

A defect in transcription results from expansion of GAA triplet repeats in the first intron of frataxin and leads to progressive spinocerebellar neurodegeneration. Cells from patients are characteristics of increased trimethylation of histone H3 and hypoacetylation of histones H3 and H4. Tretment with novel benzamide HDACi – compound 106 – increases frataxin mRNA levels, H3 and H4 acetylation and corrects the frataxin deficiency in a mouse model of Friedreich's ataxia. Both lack of acute toxicity, and a possible efficacy of this or related compounds in reverting the pathological process, support the importance of HDACi for the treatment of so far incurable neurodegenerative diseases (Rai et al., 2008).

Parkinson's disease

Parkinson's disease (PD) is the second most common neurological disorder after AD and putative causes involve mutations in several proteins, including α-synuclein. This protein binds histone H3 in vivo and when it is overexpressed, α-synuclein induces H3 hypoacetylation. Accordingly, histone acetylation ameliorates α-synuclein toxicity. SB and vorinostat diminished apoptotic cell death and rescued dopaminergic neuron degeneration in transgenic flies models of PD. More recently, benefical effects of SIRT2 inhibition were identified. In vitro studies revealed that SIRT2 inhibitors increase acetylation of α-tubulin and accumulate large α-synuclein aggregates which appear to be protective whereas small aggregates correlate with toxicity. Even though the precise mechanism of HDACi protection remains unclear, there may be therapeutical benefit of SIRT2 treatment in PD and other diseases where aggregation of misfolded proteins is central to disease pathogenesis (Hahnen et al., 2008).

Psychiatric disorders

It has been demonstrated that depression is associated with chromatin remodelling and overexpression of HDAC5 which can be reversed by chronic antidepressant hyperacetylation (Tsankova et al., 2006). Similarly, SB shows antidepressant-like effects in mice (Schroeder et al., 2007). These experiments underscore the therapeutic potential for histone methylation and deacetylation inhibitors in the treatment of depression and other psychiatric disorders

Chromatin remodelling may also play an essential role in the other cognitive disorders, for instance schizophrenia, drug addiction and anxiety disorders. Animals treated with HDACi showed induced sprouting of dendrites, an increased number of synapses, and reinstated learning behaviour and access to long-term memories (Kazantsev and Thompson, 2008).

Rett syndrome

Rett syndrome is an X-linked dominant neurodevelopmental disorder, one of the most common causes of mental retardation in females. It is caused by mutation in the gene (MECP2) encoding methyl-CpG-binding protein 2 which mediates transcriptional repression through interaction with histone deacetylases (Amir et al., 1999). Future studies exploring the therapeutic potentials of specific HDACi are expected in this disorder.

Rubinstein-Taybi syndrome

Deletion or mutation of the histone acetyltransferase CBP or in rare cases the mutation of its close homolog p300 are the causes of Rubinstein-Taybi syndrome (RSTS). This autosomal dominant mental disorder is characterized by below-average intellectual function, postnatal growth deficiency, microcephaly and skeletal abnormalities. Long-term memory impairment is associated with histone hypoacetylation in the hippocampi of affected mice and can be restored by pan-HDACi vorinostat injections before training in behavioral studies. Simultaneously, behavioral tests revealed impaired stabilization of short-term and long-term memory in mice lacking HAT activity and these defects were reversible by administration of TSA before training. Since SB and TSA manifest enhanced long-term memory formation also in non-diseased animals, HDACi treatment might represent a promising route also for the treatment of disturbances in memory formation such as age-related memory impairment (Hahnen et al., 2008).

6 Experimental part

6.1 Materials

~~3.1.1~~6.1.1   Animals

Primary cultures were generated from the offspring of Wistar rats (CRIFFA, Barcelona, Spain). Handling and care of animals were conducted according to the European Union guidelines for animal research (86/609/EEC; in agreement with the NIH guidelines) and Portuguese law (Portarias nº. 1005/92 and nº. 1131/97).

~~3.1.2~~6.1.2   Reagents

Culture media and supplements (Invitrogen)
Cytosine arabinoside – AraC (Sigma)
FURA-2 AM (Invitrogen, Carlsbad, CA)
MTG – mitotracker green (Invitrogen, Carlsbad, CA)
Polyethylenimin (Sigma)
Trichostatin A (Sigma)
Other reagents were purchased from Sigma-Aldrich unless otherwise specified

~~3.1.3~~6.1.3   Solutions

DMEM - Dulbecco's Modified Eagle's Medium (Sigma)
HBSS Buffer - Ca^{2+}- and Mg^{2+}-free Hank's balanced salt saline
Krebs Ringer Buffer (KRB)
In mM: 1.3 $CaCl_2$, 1 $MgCl_2$, 15 glucose, 135 NaCl, 20 HEPES, 5 KCl, 0.4 KH_2PO_4, pH 7.4
Neurobasal medium (NBM, Invitrogen ,Carlsbad, CA)
supplemented with 1% glutamax,
2% B27 (Brewer et al., 1993)
1% FBS – fetal bovine serum
100 U/ml penicillin

and 0.1 µg/ml streptomycin

~~3.1.4~~6.1.4 Tools and equipment

24 – well chamber, 22-mm-diameter glass coverslips

Dissecting surgical material – tissue forceps, tweezers

Neubauer chamber, slides

Vertical Laminar Flow Chamber (BSC, FASTER)

Horizontal Laminar Flow Chamber (Hera guard, Heraeus)

Incubator fo cell cultures (Hera cell 150, Heraeus)

Refrigerated Centrifuge (5810R, Eppendorf)

Steremicroscope (Stemi DV4, Zeiss)

Phase Contrast Inverted Microscope (TMS, Nikon)

An inverted epifluorescence microscope (Eclipse TE300; Nikon, Tokyo, Japan) equipped with 20, 40 and 60× air objectives)

Monochromator (Polychrome II; TILL Photonics, Martinsried, Germany)

CCD camera (C6790; Hamamatsu Photonics, Hamamatsu, Japan)

Temperature controller (TC-324B, Warner Instrument Corporation)

analysis software:

Aquacosmos 2.6, Hamamatsu Photonics

ImageJ (available at http://rsb.info.nih.gov/ij/, written by W. Rasband at the National Institutes of Health) with special plug-in MtrackJ (available at http://rsb.info.nih.gov/ij/track/track.html)

GraphPad (San Diego, CA) Prism 5.0.

6.2 Methods

6.2.1 Neuronal culture

Preparation of the culture

We used primary cortical and striatal cultures derived from embryonic day 17 (E17) to E19 rat pups. Cultures were prepared similarly to previously described

procedures (Oliveira et al., 2006; Oliveira and Gonçalves, 2009). The embryos were decapitated directly after removing from pregnant females (euthanized under deep isofluorane anaesthesia) and the brains were rapidly taken out and placed in a petri dish half-filled with ice-cold sterile HBSS Buffer.

Hemi-cortices (free from meninges, olfactory bulbs, hipocampus, and subcortical nuclei) and hemi-striata were carefully excised under a dissecting microscope, pooled according to brain region into another dish containing ice-cold HBSS, and processed in parallel (sister cultures). At first, brain regions were minced and dissociated with 0.25% trypsin-EDTA. After enzym inhibition by 10% FBS in DMEM, the suspension was centrifuged for 5 min at 300 g (1,200 rpm) at 4 °C. The supernatant was aspired and pellets were resuspended in the fresh DMEM and filtered through cell strainers (pore size 40 µm) to avoid cell aggregates. Cells were counted in Neubauer chamber, using Trypan Blue to exclude dead cells (typically under 10 %), and plated in polyethyleneimine-coated glass-coverslips distributed in 24-well chambers at a density of 10^5 cells per coverslip, 0.5 ml of Neurobasal medium (NBM) per chamber, respectively.

Cultures were maintained at 37°C in a humidified atmosphere of 5% CO_2/95% air. After 24-48 h, when cells begun sprouting, cytosine arabinoside (10mM) was added to inhibit proliferation of noneuronal cells. Medium was changed every 3-5days.

Coating coverslips

Sterilized glass round cover-slips (12mm) were positioned into 24-well chamber, coated with 0.5 ml polyethylenimin per well, prevented from floating and incubated at 37°C overnight. In the day of experiment, second coating was proceeded with 10% FBS in NBM solution, supplemented with 100 U/ml penicillin and 0.1 µg/ml streptomycin, 0.5 ml per well, and incubated for 1 hour at 37°C. Cells were plated on aspirated and dried coverslips.

~~3.2.2~~6.2.2   Treatment

Single concentration of TSA was chosen in preliminary experiments on the basis of "maximal effective concentration devoid of any obvious toxicity." Both, cortical and

striatal cells were incubated with 50 nM TSA for 3-7DIV and used in experiments (Oliveira et al., 2006).

Concentration of TSA is one-half of the maximal used without toxic effects in cerebellar granule neurons, tested by Kanai et al. (2004) during 7 DIV incubation time to show the maximal protection from excitotoxicity. Ajamian et al. (2004) indicates those concentrations as being even lower than those reported as "subapoptotic" in other neural cell lines. Moreover, TSA effectively increased histone acetylation even at lower concentrations (Oliveira et al., 2006).

All functional experiments were performed without HDAC inhibitors in the loading and assay buffers.

6.2.3 Movement analysis

We used 10-14 DIV cells in functional imaging experiments. Cells were simultaneously loaded with two probes: mitotracker green (MTG) (40nM) and FURA-2 (4μM). MTG stains mitochondria selectively with bright green fluorescence, being excited at 488nm. FURA-2 is a ratiometric fluorescent calcium indicator and it is excited at 340 and 380nm. Cells loaded with probes were incubated in the prewarmed medium under appropriate growth conditions, 30-45 minutes prior to experiments. After the incubation period, coverslips were washed by KRB buffer three times in the plastic chamber and another three times in the microscope chamber. This procedure was carried out promptly to prevent cells from drying.

Coverslips mounted in a nonperfused 500 μl chamber were thermostatized at 37°C. Experiments proceeded near the room temperature do not test the neuronal functions at the physiological conditions and show substantial differences in results, e.g. presynaptic functions in primary rat cultures (Micheva and Smith, 2005) and at higher temperatures, accurate fluorescence imaging in long-term experiments is compromised. Images were obtained at 340nm, 380nm and stacks of 120 images (frequency of one frame per 5 s) were acquired at 488 nm wavelength.

For each experiment, we analyzed 3-4 independent regions of cover slip to avoid cells from long-term exposure of 488nm light and to obtain a more representative sampling. We used a 60x objective to obtain images containing neuronal processes with single mitochondria resolution, and 20x objective to precisely determine the direction of

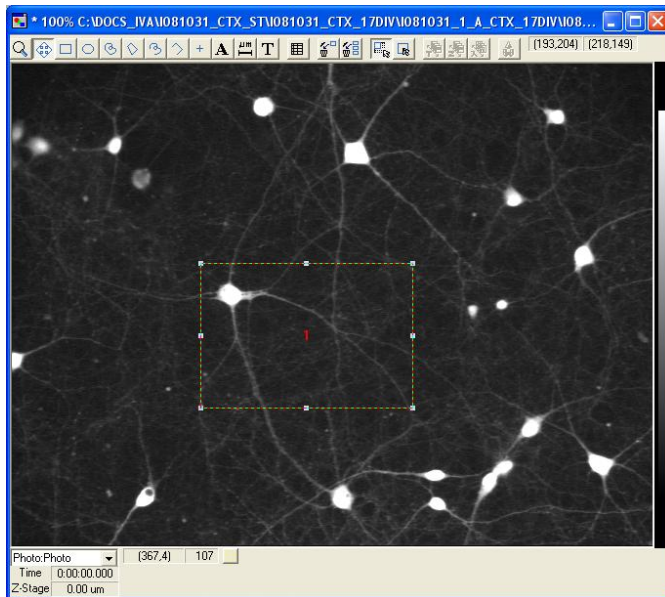movement (antero/retrograde) according to the location of processes relative to the cell body (Fig. 11).

Figure 11 Cortical neurons at 20x magnification, 380nm (stained by FURA-2). Field inside represents the area of interest for 60x magnification and analysis of mitochondrial trafficking.

Manual analysis

Two approaches to identify an alteration of the mitochondrial movement were used. At first, we studied mitochondrial movement velocity by using MTrackJ – plug-in of ImageJ analysis software. Particular mitochondria of each field, represented in the real time image video converted to Grayscale, were tracked during its motion.

We selected mitochondria moving "smooth" or "stop and go" (see Theoretical part – patterns of mitochondrial movement), both elongated and rounded, and we traced them from the first frame they had appeared in the movie field to the last. Our criterion was to choose 10 mitochondria covering the largest distances during the movie, typically corresponding to the fastest moving in a single direction. The time and the distance that mitochondrion traveled in neurite or spent in stationary state was recorded (Fig.12).
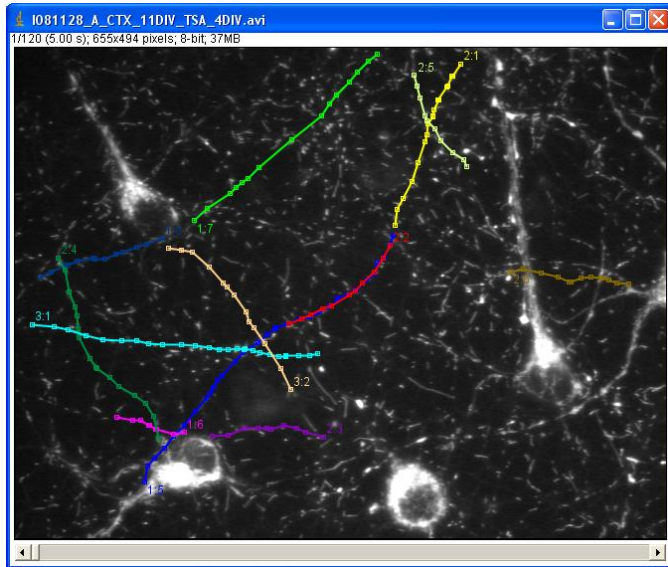
45

Figure 12 Tracks of mitochondria made with MTrackJ. The 488nm image of particular field was tracked and tracks were divided into three clusters (first number of the track name) according to direction of the movement.

We created three clusters to distinguish retrograde, anterograde and undetermined direction of movement. This last cluster comprised those mitochondria that we could not positively ascribe to anterograde or retrograde due to the complexity of the neuronal connections in which they travelled.

Velocity of the movement was calculated by dividing the distance over time for every step in which mitochondria moved. Using a similar strategy to Trushina et al. (2004), only parts of the total track with the velocity >0.18 μm/s were considered as "moving" and included into average movement speed (Fig. 13). To express speed in standard units, we used the formula 1px = 0.27 μm (derived from micrometer calibrated images acquired in our imaging system).We marked the average movement speed for each of observed fields.
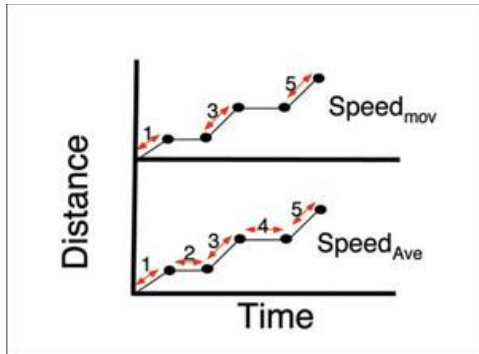
Figure 13 Difference between average speed (Speed$_{ave}$) and speed of the movement (Speed$_{mov.}$) (Trushina et al., 2004). Speed$_{ave}$ is calculated as an average of every single speed during the presence of mitochondria in the movie. Speed$_{mov}$ average does not include velocities calculated when mitochondrion stop (velocity between two measured points <0.18 μm/s).

Semi-automatic analysis

Another approach of studying mitochondrial movement was to measure overall dynamic movement mitochondria in the field and to convert this result per single mitochondrion. Images were acquired within the same condition as using manual analysis.

We projected in ImageJ the stack of 120 movie images into one projection – image that was divided by one single image of that movie. The result (32bit) was converted to black and white images by double using the Threshold function with the parameter Set background pixels to NaN selected for the first applying. Final image was skeletonized (Fig.14) and the value of total dynamic movement was expressed by image histogram.

Value of the mitochondrial portion in the field was also measured in ImageJ software, using the more precise Rolling Ball plugin (with 22 diameter, background correction) in Aquacosmos. Image of mitochondria was thresholded as previously, with the manual control and comparison with the original movie, and using the Regions of interest (ROI) Manager, we erased all non-mitochondrial particles (cell bodies, and saturated sections of images). The skeletonized image (Fig.15) histogram was then compared with the value of dynamic movement histogram. Results were analyzed as an average for each coverslip.
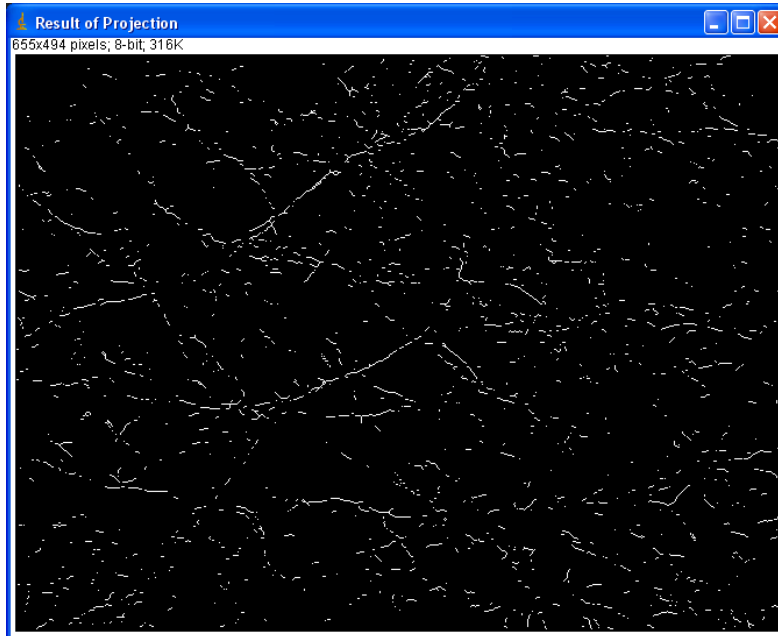
Figure 14 Skeletonized thresholded image of dynamic movement in the movie (projection divided by single image of mitochondria).
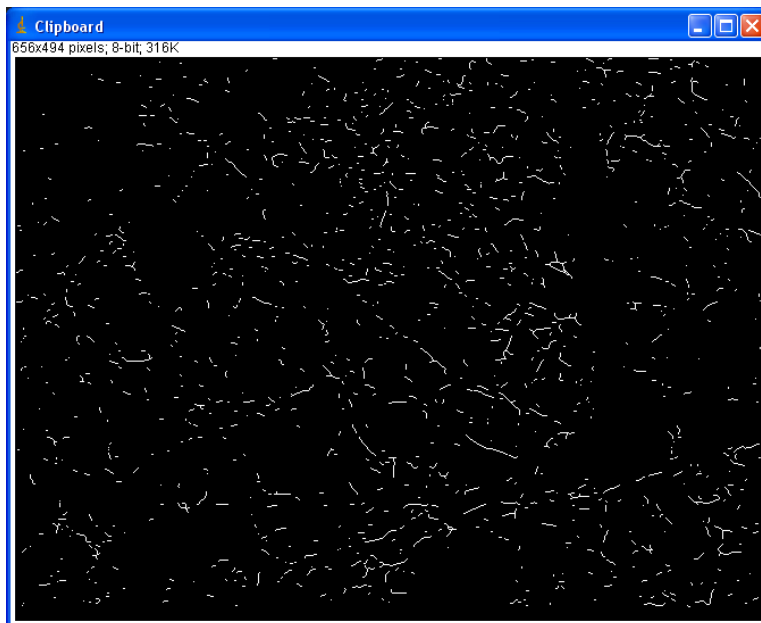

Figure 15 Skeletonized thresholded image of mitochondria (488nm) without cell bodies.
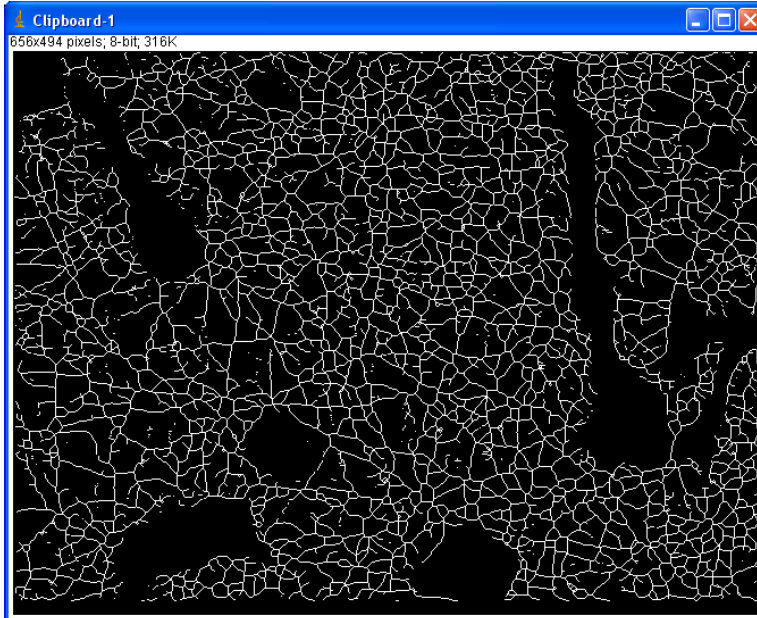
Figure 16 Skeletonized thresholded image of neuronal processes (380nm) without cell bodies.

6.2.4 Mitochondrial fractional occupancy

Mitochondria fractional occupancy expresses the percentage of the total neuronal processes length that is occupied by mitochondria. Histogram of the image presenting the total mass of mitochondria (Fig.15) was divided by histogram of the 380 nm image presenting neuronal processes (Fig.16) and this proportion stands for fractional occupancy (total mitochondrial length/process length). We processed 380 nm images by the procedure described previously for mitochondria images, using the same ROI.

6.2.5 Calcium levels

Calcium levels are expressed by the ratio of 2 wavelengths images – 340 and 380nm made in Aquacosmos. Both of them were corrected with Rolling Ball (diameter 22), and divided by Ratio calculation program. Image of 340nm was used to define background, intensity level was manually set according to the value of blank fields of

49

the image. Noise filter and zero clip were applied. We calculated ROIs without the cell bodies (Fig.17).
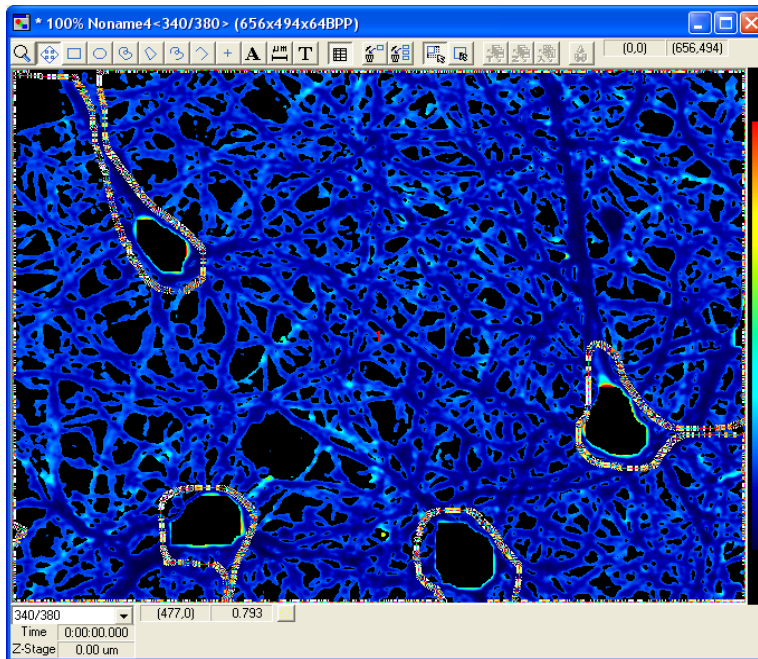

Figure 17 ROIs of ratio 340/380 nm – calcium levels.

6.2.6 Statistics

Differences among group means were assessed with ANOVAs using GraphPad Prism 4.0 (San Diego, CA). Differences for all statistical tests were considered statistically significant when $p > 0.05$.

7 Results

7.1 Analysis of mitochondrial movement in isolated vs. connected neurons

Isolated neurons are best for identifying neuronal processes belonging to the same neuron, and thus to identify primary and secondary branching, as well as anterograde and retrograde mitochondrial movement. However, isolated neurons, likely because they have few synapses, could display very low mitochondrial movement.

Previously to each experiment, we explored the coverslip using 20x magnification to select the region of healthy neurons with well-established connections. We assume that stimuli from surrounding neurons support active mitochondrial trafficking and their cooperation.

To test this hypothesis, we manually analysed mitochondrial trafficking in an isolated cortical neuron in comparison to one which was closely connected to other neurons. In the processes of isolated neurons, very few mitochondria moved smoothly and even those exhibited considerably lower average speeds than those in connected neurons (Fig. 18).

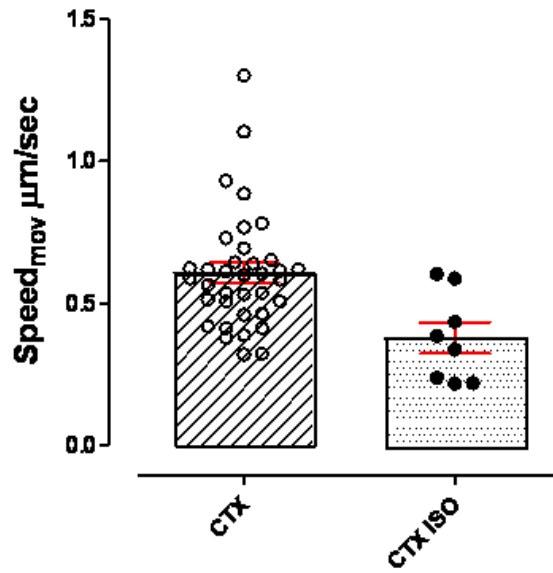**Figure 18 Total fraction of moving mitochondria and their mean velocities decrease in isolated neurons.** We show that portion of moving mitochondria and average speed velocity of cortical mitochondria are lower in an isolated neuron (CTX ISO) than in a neuron with processes connected to a network (CTX). Each circle represents average speed of single mitochondria. Column bars represent average, while error bars in red are S.E.M.

7.2 Comparison of mitochondrial trafficking in cortical vs. striatal neurons and the effect of HDAC inhibition, by manual analysis.

7.2.1 Comparison between anterograde and retrograde mitochondrial movement in cortex and striatum

In the course of studying mitochondrial movement, the first characterization of mitochondrial trafficking was done manually monitoring single mitochondrion. This method allows us to distinguish the direction of movement (anterograde vs retrograde) and see if mitochondrial velocities in cortex and striatum, both control and TSA treated, differ depending on the direction of the movement.

We created clusters of measured tracks of mitochondria in axons and dendrites and those were divided accordingly to direction of movement. Average speeds of all included mitochondria were calculated for both clusters independently (Fig. 19).

	CTX_10DIV			CTX_10DIV_TSA_3DIV			ST_10DIV			ST_10DIV_TSA_3DIV		
	A	B	C	A	B	C	A	B	C	A	B	C
Fractional occupancy	49.38	28,29	NA	31,36	26,07	44,61	45,23	42,89	53,31	46,12	33,14	47,64
Calcium 340/380 ratios	0,9730	0,9379	0,9619	0,8682	0,8832	0,9057	0,8252	0,8457	0,8410	0,8332	0,8475	0,8108
Dynamic movement	12789	6782	6846	6945	9033	6412	11544	7086	11466	9347	14061	8900
Dynamic/mito	0,8762	0,8763	0,3559	0,6482	0,5513	0,3322	0,4746	0,4928	0,5061	0,552619	1,050504	0,760
Av mov speed (>0.18)um/s												
Anterograde (cluster1)	0,651	1,157	0,371	0,745	0,579	0,767	0,447	0,32	0,386	0,72	0,6	0,499
	0,494	0,952		0,65	0,597		0,333	0,473		0,409	0,673	0,633
	0,499	0,799		0,754	0,505		0,298	0,334		0,831		0,724
	0,554	0,542		0,688	0,554		0,559	0,723				0,59
		0,468			0,526		0,559	0,578				
		0,488			0,786			0,559				
					0,675			0,456				
Retrograde (cluster2)	0,675	1,044	0,676		0,597	0,846	0,713	0,347	0,57	0,62	0,66	0,811
			0,708	0,748	0,535	0,544	0,417	0,471		0,494	0,741	0,75
				0,458	0,395	0,558				0,717	0,418	0,55
				0,857	0,718	0,85						
						0,73						
						0,775						
						0,698						
						0,706						
unknown (cluster3)	0,523	0,538	0,518	0,669	0,667	0,611	0,496	0,498	0,384	0,743	0,571	0,579
	0,43	0,531	0,443	0,836	0,725	0,462	0,342	0,286	0,307	0,743	0,71	0,55
	0,435	0,576	0,544	0,596	0,839			0,32	0,319	0,605	0,864	0,585
	0,832	0,468	0,657						0,404	0,933	0,593	0,492
	0,545	0,561	0,526						0,489	0,694	0,984	
	0,566	0,615	0,438						0,563	0,574		
		0,757	0,509						0,511			
		0,771	0,463						0,638			
Global Average	0,564	0,684467	0,532091	0,7001	0,621286	0,686091	0,462667	0,447083	0,4571	0,673583	0,6814	0,614818
Anterograde Average	0,5495	0,734333	0,371	0,70925	0,603143	0,767	0,4392	0,491857	0,386	0,653333	0,6365	0,6115
Retrograde average	0,675	1,044	0,692	0,687667	0,56125	0,713375	0,565	0,409	0,57	0,610333	0,606333	0,703667

Figure 19 Table of analysis for an individual experiment. We compared cortical (CTX) and striatal (ST) cultures, age 10 DIV, and the same cultures treated with TSA (50nM) for 3 DIV. Average speed in movement > 0.18μm/sec (Av mov speed) was measured in 3 random fields of each coverslip.

Anterograde and retrograde moving mitochondria were divided into clusters, unknown cluster was created for tracks with undetermined direction of movement. We calculated average movement speed for each coverslip, differentiating direction of movement as well, and mean values were processed in graphs. Table shows groups of particular velocities reached by single mitochondrion and by analysis of the average values. Cortical mitochondria transport occurs at higher average speed vs. striatal and TSA treatment enhanced average mitochondrial velocity in striatum, but not or only slightly in cortex. Fractional occupancy, calcium levels, dynamic movement and dynamic movement per mitochondrion are adressed in the next sections.

In cortex, we compared anterograde and retrograde movement in both control and TSA (50nM, 3 DIV) treated samples and the average speeds as well as dynamics of movement were similar (Fig. 20). We did not notice that TSA could improve neither impair mitochondrial trafficking in specific movement direction. There are very few mitochondria going retrogradely, as in fact retrograde movement comprises minor fraction of trafficking mitochondria (Chang and Reynolds, 2006b).

Figure 20 Anterograde and retrograde mitochondrial movement in cortical neurites are equivalent. TSA does not increase mitochondrial trafficking velocities in cortical neurons in anterograde nor retrograde direction of movement. We present data from a single experiment where the direction of mitochondrial movement in cortical neurons (CTX) 10 DIV was identified. Each circle represents a single mitochondrion, column bars and error bars are average speed ± SEM. Average mitochondrial speed is equivalent in anterograde (ANT) and retrograde (RET) direction of movement. TSA (50nM, 3 DIV) treatment does not affect anterograde nor retrograde average speed levels.

Similarly to cortical mitochondria, striatal mitochondria also move with identical average speed in both directions (Fig. 21). TSA (50nM, 3 DIV) treated cultures exhibited significantly higher average mitochondrial speeds (which was further confirmed in the next results section). However, both anterograde and retrograde average velocities increased to the same level.

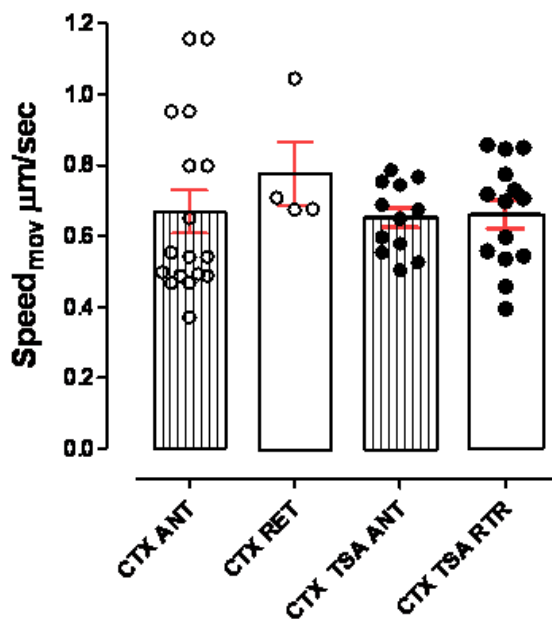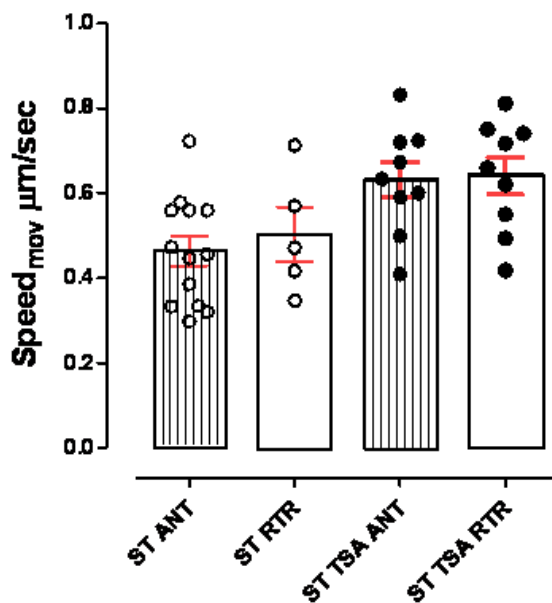**Figure 21 Anterograde and retrograde mitochondrial movement in striatal neurites are equivalent. TSA increases mean mitochondrial velocities in both anterograde and retrograde movement direction.** We present data from single experiment where the direction of mitochondrial movement in striatal neurons (ST) 10 DIV was distinguished. Each circle represents average speed of single mitochondria, column bars and error bars are average speed ± SEM (in red). Average mitochondrial speed is equivalent in anterograde (ANT) and retrograde (RET) direction of movement. TSA (50nM, 3 DIV) treatment increased both anterograde and retrograde average velocities of striatal neurons.

Given the absence of differences in anterograde and retrograde movement speeds, the following results are presented in combination and without specifying the direction of movement. Moreover, that absence of differences suggested that semi-automatic analyses (without identifying anterograde and retrograde movement) might provide faster but still reliable measurements.

7.2.2 Comparison of mitochondrial trafficking in cortical vs. striatal neurons and the effect of HDAC inhibition

We next analyzed 3-5 independent cultures for each group of neurons to describe the differences between cortical and striatal mitochondrial average velocities and to determine the effect of TSA treatment (Fig 22).

Cortical mitochondria in control and TSA treated cultures moved with higher average speeds than mitochondria from striatum. This was noticed in comparison to both control and TSA treated striatal cultures, indicating that velocity of mitochondria is dependent on the brain region. According to 2 way ANOVA test, the effect of brain region is considered significant, $p < 0,05$.

Increased average speed of striatal mitochondria treated with HDAC inhibitor TSA in comparison to control suggests the potential stimulatory effect of TSA on mitochondrial movement. However, effects of TSA treatment are not significant in cortex and striatum, compared as two groups by 2 way ANOVA statistic test. The current low *n* number provides insufficient power to detect the difference, demanding further experiments in order to exclude a possible type II error (false negative).
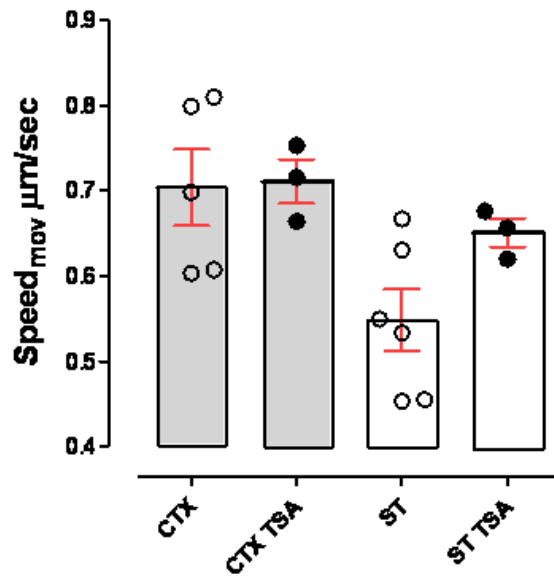
Figure 22 Cortical neurons show significantly faster mitochondrial trafficking than striatal neurons. TSA increases mitochondrial trafficking velocities in striatal but not cortical neurons. We show the levels of medium velocities of fast mitochondrial trafficking (μm/sec) in both axons and dendrites. Mitochondria from cortical control neurons (CTX), cortical neurons treated with HDACi TSA 50nM (CTX TSA), striatal control neurons (ST) and striatal neurons treated with HDACi TSA 50nM (ST TSA) were measured. Each circle substitutes mean value of mitochondrial speed in independent experiments, column bars and error bars are total average speed ± SEM. The effect of brain region is considered significant, p< 0.05.

7.3 Comparison of mitochondrial trafficking in cortical vs. striatal neurons and the effect of HDAC inhibition, by semi-automatic analysis.

Another approach of mitochondrial trafficking characterization was to describe entire mitochondrial movement, anterograde and retrograde, in axons as well as in dendrites. Therefore, we calculated the values of mitochondrial dynamics in each field with consideration to overall number of particles (Fig. 23).

Consistent with manual analysis, cortical mitochondria show significantly faster trafficking than striatal mitochondria in all of our experiments (p=0.03). These results suggest that the fraction of stationary mitochondria in cortex is lower than in striatum, or that trafficking mitochondria move for a longer distance, eventually with higher speed. Consequently, they occupy a larger area of the analyzed field, yielding an increased value of measured dynamics.

Striatum treated with TSA (50nM, 3-7DIV) exhibit faster trafficking, however the level of average dynamic movement is still lower than those for cortex and even cortex TSA treated (50nM, 3-7DIV). The effect of TSA on striatal mitochondrial movement is not so explicit as by using manual analysis, however several possible reasons for this discrepancy will be addressed in Discussion.
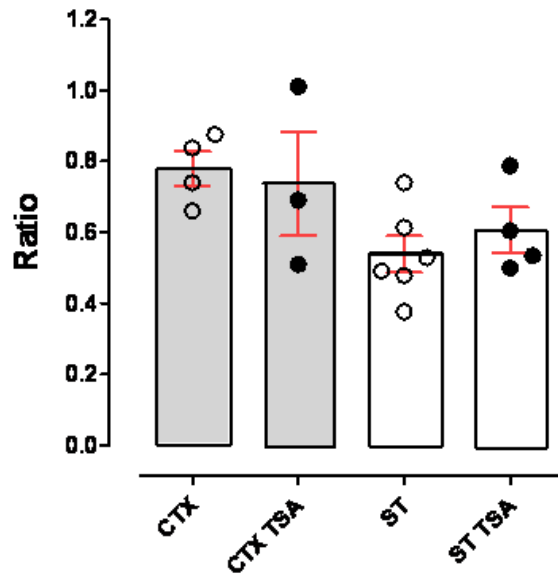
Figure 23 Cortical neurons both TSA-treated and non-treated show higher levels of overall dynamic movement than striatal neurons. TSA stimulates mitochondrial dynamic movement in striatal neurons but not in cortex. Graph represents overall dynamic movement per mitochondrion in axons and dendrites of cortical control neurons (CTX), cortical neurons treated with HDACi TSA 50nM (CTX TSA), striatal control neurons (ST) and striatal neurons treated with TSA 50nM (ST TSA). Each circle substitutes mean value of mitochondrial dynamics in independent experiments, column bars and error bars are total average speed ± SEM. Ratio is expressed in arbitrary units. The effect of brain region is considered significant, p< 0.05.

7.4 Mitochondria fractional occupancy

We have shown differences in mitochondrial trafficking between cortex and striatum, as well as the effects of treatment. Our next aim was to investigate whether these differences could be explained by variation in mitochondrial fractional occupancy.

Mitochondria fractional occupancy expresses the percentage of the total neuronal processes length that is occupied by mitochondria. High levels of fractional occupancy indicate large amount of mitochondria, and if more are actively moving at higher speeds it could increase values of mitochondrial dynamics. Nevertheless, it is also conceivable that a large mitochondria fractional occupancy might reduce the need for trafficking.

We compared cortical and striatal neurons, both treated and non-treated and calculated the fractional occupancy. Mean values of fractional occupancy in particular experiments were averaged and converted into graphs (Fig. 24).

We demonstrate that there is no significant difference between fractional occupancy of cortical and striatal neurons. Indeed, we sought to investigate whether TSA 3-7 DIV treatment influences mitochondrial fractional occupancy in cortical or striatal neurons. We made the same calculations for neurons in coverslips treated with TSA (50nM), those which undergo further dynamics analysis. Levels of fractional occupancy in TSA treated and non-treated neurons were equivalent (p=0.96). These findings exclude the possibility that differences in fractional occupancy explain differences in mitochondrial trafficking.
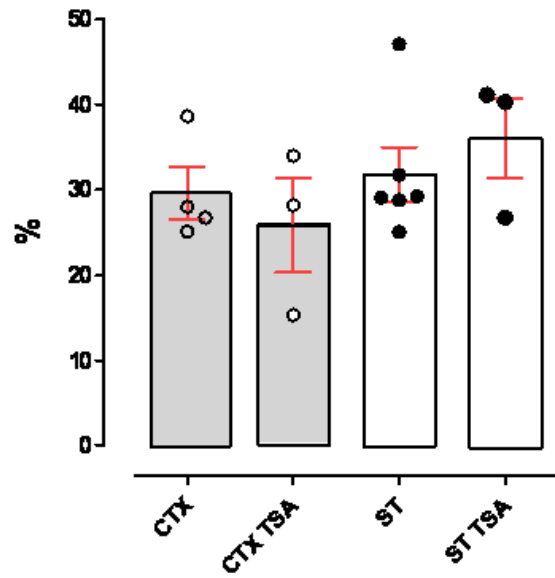
Figure 24 Fractional occupancy is similar in cortical and striatal neurons and is not affected by TSA treatment. Each circle shows average fractional occupancy from independent cultures, column bars and error bars are total average ± SEM. CTX, cortical neurons. CTX TSA, cortical neurons treated with TSA (50nM). ST, striatal neurons. ST TSA, striatal neurons treated with TSA (50nM).

7.5 Calcium concentration in neuronal processes

In addition to assesing mitochondrial fractional occupancy, we sought to explore whether the difference in mitochondrial dynamics between cortical and striatal neurons, control and TSA-treated, could be affected by differences in calcium levels in neuronal processes. Higher Ca^{2+} could drive mitochondrial trafficking to assist in Ca^{2+} buffering. Conversely, high Ca^{2+} could also stop mitochondria.

The results show a trend for lower levels of calcium in striatum in comparison to cortex (Fig. 25), suggesting this could be connected with different characteristics and vulnerability of each brain region. On the other hand, TSA treatment did not significantly change Ca^{2+} levels neither in cortical nor striatal neurons which indicate that TSA effect on mitochondrial dynamics do not correlate with alterations of Ca^{2+} levels.
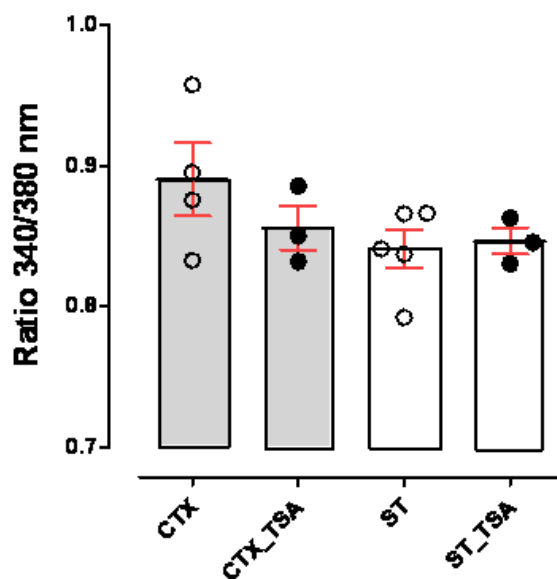
Figure 25 Cortical neurons express higher calcium levels than striatal neurons. TSA treatment does not significantly affect loads of calcium in striatal and cortical neurons. Each circle shows average fractional occupancy from independent cultures, column bars and error bars are total average ± SEM. CTX, cortical neurons. CTX TSA, cortical neurons treated with TSA (50nM). ST, striatal neurons. ST TSA, striatal neurons treated with TSA (50nM).

8 Discussion

The present study analyses mitochondrial trafficking in cortical vs. striatal living neurons and how they differ in mitochondrial fractional occupancy, trafficking speed and Ca^{2+} levels in neuronal processes. The effects of HDAC inhibitor TSA, compound used in experiments on ameliorating neurodegenerative disorders, was also monitored.

We discuss the different methods of mitochondrial dynamics analyses, used by our laboratory, their benefits and possibilities of use. In the next step, we interpret the preliminary data of our work and confront them with already elucidated or suggested findings in neurobiology. Finally, the contribution of our results and possible goals of further experiments are addressed.

During the experiments, we observed mitochondrial movement and measured speed and dynamics using manual and semi-automatic analyses. Manual tracking of individual mitochondria allows us to distinguish the direction of movement (anterograde vs. retrograde), calculate exact values of average mitochondrial speed of each single mitochondrion, thus keeping permanent control of analyzed findings. However, this method does not contain dynamics of all mitochondria in neuronal processes in the measured field, and in spite of its preciseness, manual analysis is considerably time consuming.

Semi-automatic analysis plots overall dynamics of mitochondria and at the same time acquire data on fractional occupancy. This method is very fast and more fields can be analyzed within the same time range than by manual tracking, therefore becoming more representative. However, the automation of mitochondrial trafficking analyses can introduce errors in crucial steps. For instance, mitochondria moving in the same track are all registered by only one line which notably reduces total area of mitochondrial movement in the most frequented processes - routes. In addition, it shows lower sensitivity to slight effects and demands high quality images.

According to our experience, the most practical way of general movement analysis is using semi-automatic method which reveals similar results relative to manual analysis. More precise details on mitochondria movement require a manual analysis.

First, we demonstrated why it is important to assess mitochondrial trafficking in interconnected neurons. Portion of moving mitochondria and average speed velocity of cortical mitochondria were lower in an isolated neuron than in a neuron with processes connected to a network. Isolated neurons are absent of contact with other neurons in surroundings and lack synaptic activity, which is known to require ATP supply by mitochondria. The fast mitochondrial trafficking becomes crucial if there is large energy demand in neuronal region. However, if the neuron is isolated or grows in less dense area, mitochondrial dynamics is notably lower. These results correspond to our hypothesis and sustain the aim to conduct the experiments with neurons sufficiently connected and engaged in synaptic activity and intercellular communication.

Some authors (Her and Goldstein, 2008) described axonal transport which different velocities and number of stationary particles in anterograde vs retrograde direction. Considering that tubulin acetylation recruits molecular motor proteins which are distinct for anterograde (kinesin) and retrograde (dynein) movement (Mattson et al., 2008), the HDACi could also affect these two directions differentially.

We observed axons and dendrites together and mitochondrial trafficking speeds did not differ in either anterograde or retrograde direction. Moreover, TSA treatment showed the same effect in both directions for cortex and striatum which was in agreement with other experiments observing vesicle trafficking (Dompierre et al., 2007), suggesting a general role for microtubule acetylation and possible interferences with both anterograde and retrograde protein motors. In consequence of these findings, we applied semi-automatic analysis assessing mitochondrial dynamics in combined direction.

Our main task was to describe and compare mitochondrial trafficking in cortex and striatum and evaluate the effect of HDAC inhibition. Statistic analyses of our results revealed that mitochondrial average speeds as well as total dynamics are significantly higher in cortex than in striatum. Lower mitochondrial trafficking in striatum could contribute for its greater vulnerability in comparison to other brain regions. Striatum is more susceptible to ψ_m depolarization, respiratory defects and abnormal $[Ca^{2+}]_i$ homeostasis. It has been previously demonstrated by our laboratory that mitochondrial Ca^{2+} buffering capacity is decreased in striatal neurons and astrocytes comparing them with cortical neurons and astrocytes (Oliveira and

Gonçalves, 2009). This likely contributes to selective striatal vulnerability in pathologies such as HD and other neurological disorders.

Our data also show the trend of increased mitochondrial trafficking in striatal neurons as a result of HDACi treatment. Neuroprotective effect of TSA by inhibiting the HDAC1 enzyme has been previously described (Dompierre et al., 2007), as well as its promising experimental use in neurodegenerative disorders therapy (see Theoretical part). However, the neuroprotective mechanisms associated to TSA treatment are not fully understood. DNA-demethylation, altered immune responses, enhanced protein degradation pathways and cytoskeletal function modulating are the most probable effects of HDACi treatment that have been suggested (Hahnen et al., 2008; Kazantsev et al., 2008).

Our preliminary results lead to a possible explanation of HDACi therapeutical effects, which is mitochondrial dynamics increasing. Average mitochondrial speeds as well as overal movement were increased in TSA treated striatal neurons in comparison to control neurons. By analysing mitochondrial fractional occupancy, we determined equivalent portion of mitochondria in all tested neurons. Thus, the different amount of mitochondria and its possible influence on mitochondrial movement were excluded.

Increased Ca^{2+} levels were measured in cortical neurons that show more dynamic movement in our experiments than striatal neurons. However, calcium concentrations in neuronal processes of control and HDACi treated neurons were similar in spite of enhanced mitochondrial dynamics in TSA treated striatum. Consequently, effect of TSA seems to be independent of Ca^{2+} levels.

The possible mechanism of TSA effects on enhanced mitochondrial trafficking is the acetylation of lysine 40 of α-tubulin. TSA, non-selective HDACi, act on HDAC6 (Haggarty et al., 2003) which interacts with and deacetylates tubulin and microtubules in vivo (Zhang et al., 2003). α-tubulin acetylation influences the binding and motility of kinesin-1 and pharmacological treatments such as TSA cause a redirection of kinesin-1 transport by increasing microtubule acetylation (Reed et al., 2006). By this mechanism, HDACi could control motor-protein trafficking along microtubule tracks.

Dompierre et al. (2007) have demonstrated that HDACi, including TSA, increase vesicular transport of BDNF by inhibiting HDAC6 and thereby increasing acetylation of α-tubulin. We focused on trafficking of fundamental cell organelles -

mitochondria, and show the same trend of increased transport depending on TSA treatment.

On the other hand, some studies exhibit benefical effects of HDAC6, hence its inhibition is not clearly profitable for degenerating neurons. We need to consider all possible undesirable side consequences of HDACi very carefully because HDAC6 functions are presumably far more than just as a deacetylase. For instance, authophagic degradation of aggregated proteins require intact microtubule skeleton and HDAC6. This deacetylase binds both polyubiquitinated misfolded proteins and dynein motors, ensuring transport of toxic aggregates to aggresomes (Iwata et al., 2005; Kawaguchi et al., 2003).

However, novel findings indicate that HDAC6 interacts with the microtubule-associated protein tau (which forms neurofibrillary tangles in AD). Interestingly, this interaction is not disrupted by either TSA or the selective HDAC6 inhibitor tubacin, supporting the hypothesis that cell responses to abnormal protein aggregation is not dependent on HDAC6 acetylation (Ding et al., 2008).

Despite the fact that HDAC activity inhibition has been shown to protect neurons from neurodegeneration (Kanai et al., 2004; Pandey et al., 2007), or block neuronal loss in Drosophila and mouse models of HD, there are reports showing that treatment of cerebellar granule neurons with HDACi actively induces apoptosis. The contradictive effects of HDACi can be explained by the tissue and stage-specific expression of different classes of HDACs (Morrison et al., 2007).

Our future interest is in analysing mitochondrial trafficking in neurodegenerative disease models (e.g. HD, AD, …). It has been already shown that mutant huntingtin aggregates impair mitochondrial trafficking in cortical neurons, interacting with cytoskeletal components and molecular motors (Chang et al., 2006). Moreover, tubulin acetylation is reduced in HD brains (striatum) and TSA compensates for the transport- and release-defect phenotypes that are observed in disease (Dompierre et al., 2007). We would like to discover the effects of HDACi directly on mitochondria.

No significant trafficking alteration was found in wild cortical neurons treated with TSA. However, subsequent crucial question is whether TSA could improve mitochondrial trafficking in cortex impaired by neurodegenerative disease, as it was described in striatum. We can also speculate that there could be some average speed

limit, already reached during physiological conditions by cortical mitochondria, thus HDACi effects would reveal only in impaired neurons.

Another aim would be to test other HDACi and analyse their effects on mitochondrial trafficking. We are particularly interested in results of tubacin treatment, selective HDAC6 inhibitor, which could help to elucidate the mechanism of HDACi activity. However, effects of other HDACi, e.g. class I-selective VPA, well-established neurological drug, would be worthy.

SIRT2 protein, class III HDAC enzyme, shows the same effect on acetylation of α-tubulin as HDAC6. Possible stimulation of mitochondrial movement by treating the neurons with SIRT2 in further experiments, could be additional clue to prove our previous hypothesis (increase of mitochondrial speeds in dependence on α-tubulin acetylation), and in addition this could be the next step to describe and understand mitochondrial trafficking in living neurons.

9 Conclusion

In our experiments, we aimed to explore mitochondrial trafficking in living neurons. Our data provide evidence that striatal mitochondria move with lower average speeds, exhibit decreased dynamics and contain lower Ca^{2+} levels than mitochondria in cortical neurons. It is also discussed how this could contribute to striatal particular vulnerability to neurodegeneration.

To describe the movement of single mitochondria, we used two different techniques – manual and semi-automatic analysis. We discuss the use of both of them in detailed study of trafficking. The advantages of semi-automatic analysis, its promptness and complexity, make this method preferred for overall analysis, as it is proposed in Discussion.

We fixed the terms of experiments with living neurons under physiological conditions, so that we analyzed only neurons with dense connection of processes. In additon, we determined no effect of mitochondrial trafficking direction on dynamics and average speed, therefore the further experiments were focused on analysis of overal mitochondrial dynamics.

The preliminary data show the trend of increased mitochondrial average speeds in striatum as a result of TSA-treatment, independently of mitochondrial fractional occupancy and Ca^{2+} levels in neuronal processes. Accordingly, our laboratory continues in experiments with HDAC inhibition effects on mitochondrial trafficking in living neurons to bring further insight into these results.

The further intention of our work is the determination of the other HDACi (e.g. tubacin, VPA) effects on mitochondrial dynamics. We would also like to analyze mitochondrial movement and its possible HDACi-treatment alteration in neurodegenerative disease models.

10 References

Acheson et al. A BDNF autocrine loop in adult sensory neurons prevents cell death. *Nature*, 1995, vol. 374, no. 6521, pp. 450 - 453

Ajamian, F. – Salminen, A. – Reeben, M. Selective regulation of class I and class II histone deacetylases expression by inhibitors of histone deacetylases in cultured mouse neural cells. *Neurosci Lett*, 2004, vol. 365, no. 1, p. 64–68

Amir et al. Rett syndrome is caused by mutations in X-linked MECP2, encoding methyl-CpG-binding protein 2. *Nat Genet*, 1999, vol. 23, no. 2, pp. 185-188

Anandatheerthavarada et al. Mitochondrial targeting and a novel transmembrane arrest of Alzheimer's amyloid precursor protein impairs mitochondrial function in neuronal cells. *J Cell Biol,* 2003, vol. 161, no. 1, pp. 41–54

Andersen, J. K. Oxidative stress in neurodegeneration: cause or consequence? *Nat Med,* 2004, 10 Suppl., pp. 18-25

Ankarcrona et al. Glutamate-induced neuronal death: a succession of necrosis or apoptosis depending on mitochondrial function. *Neuron*, 1995, vol. 15, no. 4, pp. 961–973.

Avila et al. Trichostatin A increases SMN expression and survival in a mouse model of spinal muscular atrophy. *J Clin Invest,* 2007, vol. 117, no.3, pp. 659-671

Biacsi, R. – Kumari, D. – Usdin, K. SIRT1 inhibition alleviates gene silencing in Fragile X mental retardation syndrome. *PloS Genet*, 2008, vol. 4, no. 3, e 1000017

Brewer et al. Optimized survival of hippocampal neurons in B27-supplemented neurobasal, a new serum-free medium combination. *J Neurosci Res,* 1993, vol. 35, no.5, pp 567–576

Butler

Calabresi, P. - Centonze, D. - Bernardi, G. Cellular factors controlling neuronal vulnerability in the brain: a lesson from the striatum. *Neurology,* 2000, vol. 55, no. 9, pp.1249-1255

Camelo et al. Transcriptional therapy with the histone deacetylase inhibitor trichostatin A ameliorates experimental autoimmune encephalomyelitis. *J Neuroimmunol*, 2005, vol. 164, no. 1-2, pp. 10-21

Carafoli et al. Generation, control, and processing of cellular calcium signals. *Crit Rev Biochem Mol Biol,* 2001, vol. 36, no.2, pp.107–260

Cardullo, R.A. - Baltz, J.M. Metabolic regulation in mammalian sperm: mitochondrial volume determines spermlength and flagellar beat frequency. *Cell Motil Cytoskel,* 1991, vol. 19, no. 3, pp. 180–188

Chang, D.T.W. – Reynolds, I.J. Differences in mitochondrial movement and morphology in young and mature primary cortical neurons in culture. *Neuroscience,* 2006a, vol. 141, no. 2, pp. 727-736

Chang, D.T.W. – Reynolds, I.J. Mitochondrial trafficking and morphology in healthy and injured neurons. *Prog Neurobiol,* 2006b, vol. 80, no. 5, pp. 241-268

Chang et al. Mutant huntingtin aggregates impair mitochondrial movement and trafficking in cortical neurons. *Neurobiol Dis*, 2006, vol. 22, no.2, pp. 388-400

Crompton, M. The mitochondrial permeability transition pore and its role in cell death. *Biochem J,* 1999, vol. 341, no. 2, pp. 233-249

Crompton et al. The interrelations between the transport of sodium and calcium in mitochondria of various mammalian tissues. *Eur J Biochem,* 1978, vol. 82, no.1, pp. 25-31

Hauke et al. Survival motor neuron gene 2 silencing by DNA methylation correlates with spinal muscular atrophy disease severity and can be bypassed by histone deacetylase inhibition. *Hum Mol Genet*, 2009, vol. 18, no. 2, pp. 304-317

Ding, H. – Dolan, P.J. – Johnson, G. V. W. Histone deacetylase 6 interacts with the microtubule-associated protein tau. *J Neurochem*, 2008, vol. 106, no. 5, pp. 2119-2130

Dompierre et al. Histone Deacetylase 6 Inhibition Compensates for the Transport Deficit in Huntington's Disease by Increasing Tubulin Acetylation. *J Neurosci*, 2007, vol. 27, no. 13, pp. 3571-3583

Erecinska, M. - Silver, I.A., Ions and energy in mammalian brain. *Prog Neurobiol,* 1994, vol. 43, no.1, pp. 37–71

Frank et al. The role of dynamin-related protein 1, a mediator of mitochondrial fission, in apoptosis. *Dev Cell,* 2001, vol.1, no. 4, pp. 515-525

Gao et al. Cloning and functional characterization of HDAC11, a novel member of the human histone deacetylase family. *J Biol Chem*, 2002, vol. 277, no. 28, pp. 25748-25755

Garesse, R. – Vallejo, C.G. Animal mitochondrial biogenesis and function: a regulatory cross-talk between two genomes. *Gene*, 2001, vol. 263, no. 1-2, pp.1-16

Gray, M.W. Origin and evolution of organelle genomes.*Curr Opin Genet Dev*, 1993, vol. 3, no. 6, pp. 884-890

Green et al. Nicotinamide restores cognition in Alzheimer's disease transgenic mice via a mechanism involving sirtuin inhibition and selective reduction of Thr231-phosphotau. *J Neurosci*, 2008, vol. 28, no. 45, pp. 11500-11510

Gregoretti, I.V. – Lee, Y.M. – Goodson, H.V. Molecular evolution of the histone deacetylase family: functional implications of phylogenetic analysis. *J Mol Biol*, 2004, vol. 338, no. 1, pp. 17-31

Guanawardena S. – Goldstein, L.S. Polyglutamine diseases and transport problems: deadly traffic jams on neuronal highways. *Neuron,* 2001, vol. 32, no. 3, pp. 389-401

Haggarty et al. Domain-selective small-molecule inhibitor of histone deacetylase 6 (HDAC6)-mediated tubulin deacetylation. *Proc Natl Acad Sci U S A,* 2003, vol.100, no. 8, pp. 4389-4394

Hahnen et al. Histone deacetylase inhibitors: possible implications for neurodegenerative disorders *Expert Opin Investig Drugs,* 2008, vol.17, no. 2, pp. 1-16

Hauke et al. Survival motor neuron gene 2 silencing by DNA methylation correlates with spinal muscular atrophy disease severity and can be bypassed by histone deacetylase inhibition. *Hum Mol Genet*, 2009, vol. 18, no. 2, pp. 304-317

Her, L.S. – Goldstein, L.S. Enhanced sensitivity of striatal neurons to axonal transport defects induced by mutant huntingtin. *J Neurosci*, 2008, vol. 28, no. 50, pp.13662-13672

Hollenbeck, P.J. – Saxton, W.M. The axonal transport of mitochondria. *J Cell Sci,* 2005, vol. 118, no. 23, pp. 5411-5419

Iwata et al. HDAC6 and microtubules are required for autophagic degradation of aggregated huntingtin. *J Biol Chem*, 2005, vol. 280, no.48, pp. 40282-40292

Kanai et al. Valproic acid inhibits histone deacetylase activity and suppresses excitotoxicityinduced GAPDH nuclear accumulation and apoptotic death in neurons. *Pharmacogenomics J*, 2004, vol. 4, no. 5, p. 336 –344

Kawaguchi et al. The deacetylase HDAC6 regulates aggresome formation and cell viability in response to misfolded protein stress. *Cell*, 2003, vol. 115, no. 6, pp. 727–738

Kazantsev, A.G. – Thompson, L.M. Therapeutic application of histone deacetylase inhibitors for central nervous system disorders. *Nat Rev Drug Discov,* 2008, vol. 7, no. 10, pp. 854-868

Khan et al. Determination of the class and isoform selectivity of small molecule HDAC inhibitors. *Biochem J,* 2008, vol. 409, no. 2, pp. 581-589

Kim et al. Defective cholesterol traffic and neuronal differentiation in neural stem cells of Niemann-Pick type C disease improved by valproic acid, a histone deacetylase inhibitor. *Biochem Biophys Res Commun*, 2007a, vol. 360, no. 3, pp. 593-599

Kim et al. Histone deacetylase inhibitors exhibit anti-inflammatory and neuroprotective effects in a rat permanent ischemic model of stroke: multiple mechanisms of action. *J Pharmacol Exp Ther*, 2007b, vol. 321, no. 3, pp. 892-901

Knott et al. Mitochondrial fragmentation in neurodegeneration. *Nat Rev Neurosci*, 2008, vol. 9, no. 7, pp. 505-518

Lee, C.W. – Peng, H.B. Mitochondrial clustering at the vertebrate neuromuscular junction during presynaptic differentiation. *J Neurobiol* , 2006, vol. 66, no. 6, pp. 522-536

Li et al. SIRT1 deacetylates and positively regulates the nuclear receptor LXR. *Cell Metab*, 2007, vol. 28, no. 1, pp. 91-106

Ligon, L.A. – Steward, O. Movement of mitochondria in the axons and dendrites of cultured hippocampal neurons. *J Comp Neurol,* 2000, vol. 427, no. 3, pp. 340-350

Liu et al. Memory loss in old rats is associated with brain mitochondrial decay and RNA/DNA oxidation: Partial reversal by feeding acetyl-l-carnitine and/or R-α-lipoic acid. *PNAS,* 2002, vol. 99, no. 4, pp. 2356-2361

Majdzadeh et al. HDAC4 inhibits cell-cycle progression and protects neurons from cell death. *Dev Neurobiol*, 2008, vol. 68, no. 8, pp. 1076-1092

Mao, L. – Wang, J.Q. Upregulation of preprodynorphin and preproenkephalin mRNA expression by selective activation of group I metabotropic glutamate receptors in characterized primary cultures of rat striatal neurons. *Brain Res Mol Brain Res*, 2001, vol. 86, no. 1-2, pp.125–137

Marzo et al. Bax and adenine nucleotide translocator cooperate in the mitochondrial control of apoptosis. *Science*, 1998, vol. 281, no. 5385, pp. 2027-2031

Mattson, M.P. – Gleichmann, M. – Cheng, A. Mitochondria in Neuroplasticity and

Neurological disorders. *Neuron*, 2008, vol. 60, no. 5, pp. 748-766

McCormack, R.M.- Denton, J.G. Role of calcium ions in the regulation of intramitochondrial metabolism. Properties of the Ca^{2+}-sensitive dehydrogenases within intact uncoupled mitochondria from the white and brown adipose tissue of the rat. *Biochem J*, 1980, vol. 190, no.1, pp. 95-105

Micheva, Kristina D. - Smith, Stephen J. Strong Effects of Subphysiological Temperature on the Function and Plasticity of Mammalian Presynaptic Terminals. *J Neurosci*, 2005, vol. 25, no.33, pp. 7481-7488

Milakovic, T. – Johnson, G. V. W. Mitochondrial respiration and ATP production are significantly impaired in striatal cells expressing mutant huntingtin. *J Biol Chem,* 2005, vol. 280, no. 35, pp. 30773-30782

Miller, K.E. – Sheetz, M.P. Axonal mitochondrial transport and potential are correlated. *J Cell Sci,* 2004, vol. 117, no. 13, pp. 2791-2804

Miller, T.A. – Witter, D.J. – Belvedere, S. Histone deacetylase inhibitors. *J Med Chem,* 2003, vol. 46, no. 24, pp. 5097-5116

Mironov, S.L. – Symonchuk, N. ER vesicles and mitochondria move and communicate at synapse. *J Cell Sci*, 2006, vol. 119, no. 23, pp. 4926-4934

Morrison, B.E. – Majdzadeh, N. – D´Mello, S.R. Histone deacetylases: focus on the nervous systém. *Cell Mol Life Sci,* 2007, vol. 64, no. 17., pp. 2258-2269

Nishizawa, Y. Glutamate release and neuronal damage in ischemia. *Life Sci*, 2001, vol. 69, no. 4, pp. 369-381

North et al. The human Sir 2 ortholog, SIRT2, is an NAD^+-dependent tubulin deacetylase. *Mol Cell*, 2003, vol. 11, no. 2, pp. 437-444

Oliveira et al. Mitochondrial-Dependent Ca^{2+}Handling in Huntington'sDisease Striatal Cells: Effect of Histone Deacetylase Inhibitors. *J Neurosci*, 2006, vol. 26, no. 43, pp. 11174-11186

Oliveira, J.M.A. – Gonçalves, J. In situ mitochondrial Ca^{2+} buffering differences of intact neurons and astrocytes from cortex and striatum. *J Biol Chem*, 2009, vol. 284, no. 8, pp. 5010-5020

Ono et al. Human cells are protected from mitochondrial dysfunction by complementation of DNA products in fused mitochondria. *Nat Genet,* 2001, vol. 28, no. 3, pp. 272-275

73

Pandey et al. HDAC6 rescues neurodegeneration and provides an essential link between autophagy and the UPS. *Nature*, 2007, vol. 447, no. 7146, pp. 859-863

Panov et al. Early mitochondrial calcium defects in Huntington's disease are a direct effect of polyglutamines. *Nat Neurosci,* 2002, vol. 5, no. 8, pp. 731-736.

Phiel et al. Histone deacetylase is a direct target of valproic acid, a potent anticonvulsant, mood stabilizer, and teratogen. *J Biol Chem*, 2001, vol. 276, no.39, pp. 36734- 36741

Pizzo, P. – Pozzan, T. Mitochondria–endoplasmic reticulum choreography: structure and signaling dynamics. *Trends Cell Biol,* 2007, vol.17, no. 10, pp. 511-517

Priault et al. Impairing the bioenergetic status and the biogenesis of mitochondria triggers mitophagy in yeast. *Cell Death Differ*, 2005, vol. 12. no. 12, pp.1613-1621

Rai et al. HDAC inhibitors correct frataxin deficiency in a Friedreich ataxia mouse model. PloS ONE, 2008, vol. 3, no.4, e1958

Reed et al. Microtubule acetylation promotes kinesin-1 binding and transport. *Curr Biol*, 2006, vol. 16, no. 21, pp. 2166-2172

Reilein et al. Regulation of molecular motor proteins. *Int Rev Cytol*, 2001, vol. 204, pp. 179-238

Reynolds et al. Mitochondrial trafficking in neurons: a key variable in neurodegeneration? *J Bioenerg Biomembr,* 2004, vol. 36, no. 4, pp. 283-286

Rosas et al. Complexity and heterogeneity: what drives the ever-changing brain in Huntington's disease? *Ann N Y Acad Sci*, 2008, vol. 1147, pp. 196-205

Rostovtseva et al. Bid, but not Bax, regulates VDAC channels. *J Biol Chem,* 2004, vol. 279, no. 14, pp. 13575-13583

Sadri-Vakili, G. – Cha, J.H. Histone deacetylase inhibitors: a novel therapeutic approach to Huntington's disease (complex mechanism of neuronal death). *Curr Alzheimer Res*, 2006, vol. 3, no. 4, pp. 403-408

Schapira et al. Mitochondrial complex I deficiency in Parkinson's disease. *Lancet*, 1989, vol. 333, no. 8649, p. 1269

Schroeder et al. Antidepressant-like effects of the histone deacetylase inhibitor, sodium butyrate, in the mouse. *Biol Psychiatry*, 2007, vol. 62, no. 1, pp. 55-64

Segretain, D. - Rambourg, A. - Clermont, Y. Three dimensional arrangement of mitochondria and endoplasmic reticulum in the heart muscle fiber of the rat. *Anat Rec,* 1981, vol. 200, no. 2, pp. 139–151

Sheehan et al. Calcium homeostasis and reactive oxygen species production in cells transformed by mitochondria from individuals with sporadic Alzheimer's disease. J Neurosc, 1997, vol. 17, no.12, pp. 4612-4622

Sheetz, M. P. Motor and cargo interactions. *Eur J Biochem*, 1999, vol. 262, no. 1, pp. 19-25

Siklós et al. Intracellular calcium parallels motoneuron degeneration in SOD-1 mutant mice. *J Neuropathol Exp Neurol,* 1998, vol. 57, no. 6, pp. 571-587

Silver, I.A. - Erecinska, M. Oxygen and ion concentrations in normoxic and hypoxic brain cells. *Adv Exp Med Biol,* 1998, vol. 454, pp. 7–16

Sun et al. Measurement of histone acetyltransferase and histone deacetylase activities and kinetics of histone acetylation. *Methods*, 2003, vol. 31, no. 1, pp. 12-23

Szebenyi et al. Neuropathogenic Forms of Huntingtin and Androgen Receptor Inhibit Fast Axonal Transport. *Neuron*, 2003, vol. 40, no. 1, pp. 41–52

Tabolacci et al. Modest reactivation of the mutant FMR1 gene by valproic acid is accompanied by histone modifications but not DNA demethylation. *Pharmacogenet Genomics*, 2008, vol. 18, no. 8, pp. 738-741

Taunton J – Hassig, CA – Schreiber, SL. A mammalian histone deacetylase related to the yeast transcriptional regulator Rpd3p. *Science,* 1996, vol. 272, no. 5260, pp. 371-372

Testa, C.M. – Sherer, T.B. – Greenamyre, J.T. Rotenone induces oxidative stress and dopaminergic neuron damage in organotypic substantia nigra cultures. *Brain Res Mol Brain Res,* 2005, vol. 134, no. 1, pp.109-118

Tsankova et al. Sustained hippocampal chromatin regulation in a mouse model of depression and antidepressant action. *Nat Neurosci*, 2006, vol. 9, no. 4, pp. 519-525

Tsuji et al. A new antifungal antibiotic, trichostatin. *J Antibiot*, 1976, vol. 29, no.1, pp.1-6

Trushina et.al. Mutant Huntingtin Impairs Axonal Trafficking in Mammalian Neurons In Vivo and In Vitro. *Mol Cell Biol,* 2004, vol. 24, no. 18, pp. 8195 – 8209

Wang, X. – Schwarz, T.L. The mechanism of Ca^{2+}-dependent regulation of kinesin-mediated mitochondrial motility. *Cell*, 2009, vol. 136, no.1, pp.163-174

Wolf et al. Traumatic axonal injury induces calcium influx modulated by tetrodotoxin-sensitive sodium channels. *J Neurosci,* 2001, vol. 21, no. 6, pp.1923-1930

Xu, W.S.- Parmigiani, R.B. – Marks, P.A. Histone deacetylase inhibitors: molecular mechanisms of action. *Oncogene,* 2007, vol. 26, no.37, pp. 5541-5552

Yoshida et al. Potent and specific inhibition of mammalian histone deacetylase both in vivo and in vitro by trichostatin A. *J Biol Chem,* 1990, vol. 265, no.28, pp. 17174-17179

Yu et al. Valproic acid promotes neuronal differentiation by induction of proneural factors in association with H4 acetylation. *Neuropharmacology*, 2009, vol. 56, no. 2, pp. 473-480

Zhang et al. HDAC-6 interacts with and deacetylates tubulin and microtubules in vivo. *EMBO J,* 2003, vol. 22, no. 5, pp. 1168-1179

Internet citation:

<http://commons.wikimedia.org/wiki/Mitochondrion>